Modelling the secular evolution of the Milky Way's disc

Hanyuan Zhang (hz420@cam.ac.uk)

with Vasily Belokurov, N. Wyn Evans, Jason L. Sanders and collaborators

University of Cambridge
Institute of Astronomy

Observational Constraints of Radial Migration in the Galactic Disk Driven by the Slowing Bar

HanYuan Zhang[1], Vasily Belokurov[1], N. Wyn Evans[1], Jason L. Sanders[2], Yuxi(Lucy) Lu[3,4], Chengye Cao[5], GyuChul Myeong[1], Adam M. Dillamore[2], Sarah G. Kane[1], and Zhao-Yu Li[5,6]

Orbital migration and heating history of the Galactic disc: a transition between the bimodal discs

HanYuan Zhāng,[1★] Vasily Belokurov,[1] Jason L. Sanders,[2] N. Wyn Evans,[1] David Chemaly,[1] Daisuke Kawata,[3] Natsuki Funakoshi,[3] Neige Frankel,[4,5] Sarah G. Kane,[1] and Sergey E. Koposov[6,1]

Enhanced rates of stellar radial migration in gas-rich discs at high redshift

HanYuan Zhāng,[1★] Thor Tepper-García,[2] Vasily Belokurov,[1] N. Wyn Evans,[1] Takafumi Tsukui,[3] Hillary Davis,[2] Joss Bland-Hawthorn,[2] Jason L. Sanders,[4] Oscar Agertz[5]

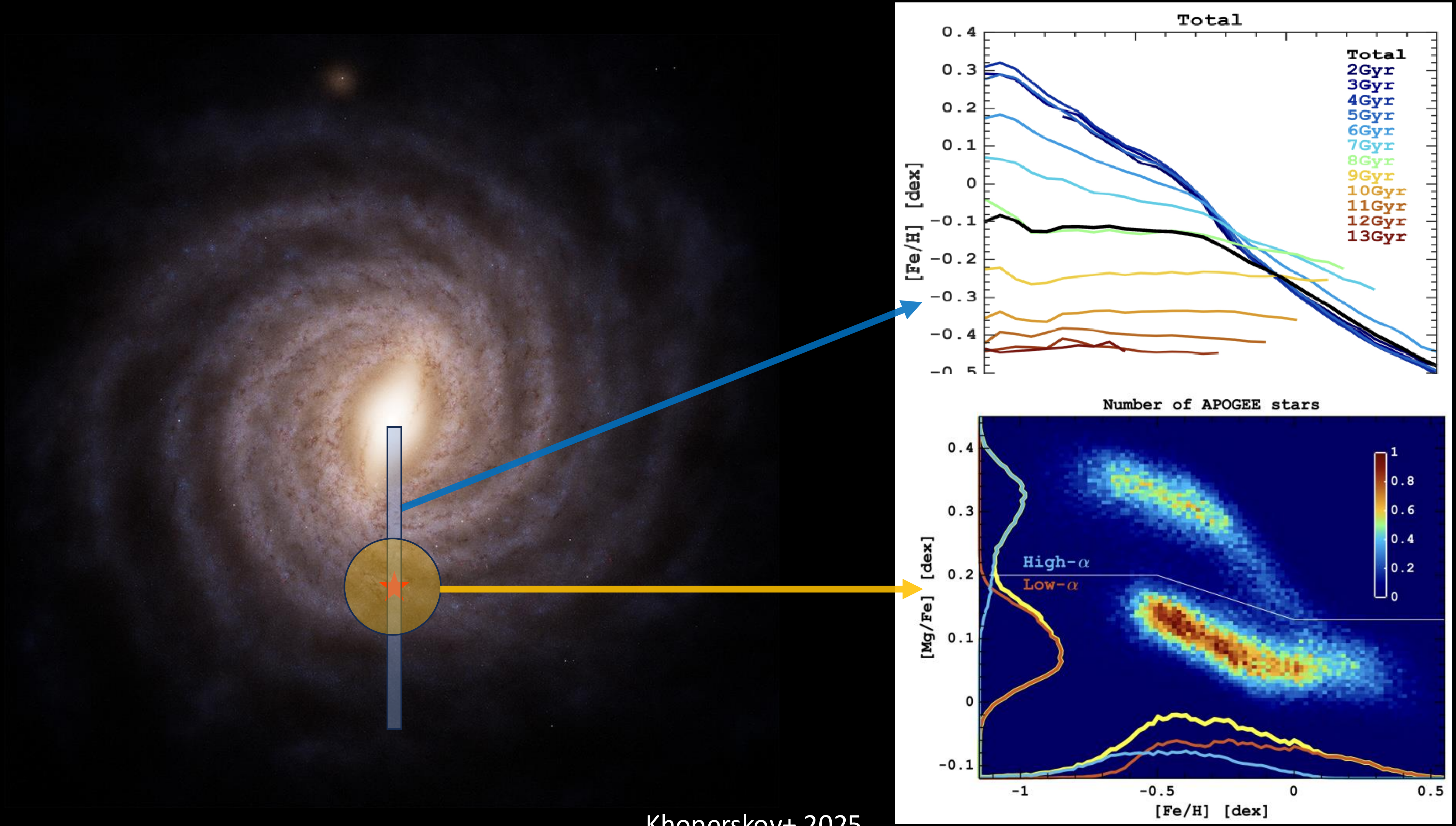

Khoperskov+ 2025

Galaxies at high$-z$

van der Wal & Meidt 2025

- Disc substructures (like bar and spiral) already appeared at the early time of the Universe

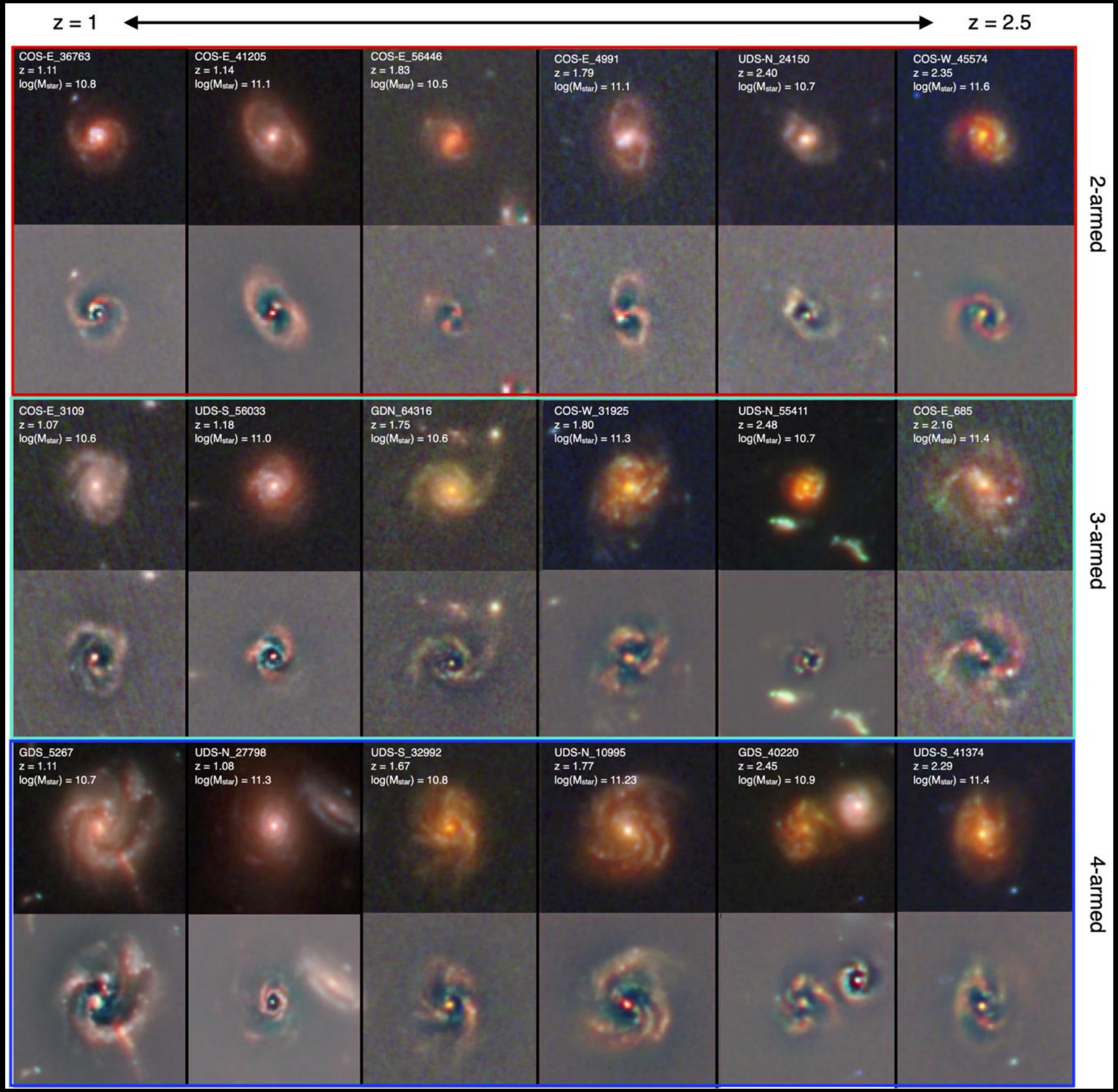

See also Ferreira+23, Kuhn+24, Espejo Salcedo+25 etc.

Galaxies at high$-z$

Tsukui et al. 2025

- Disc substructures (like bar and spiral) already appeared at the early time of the Universe

- Tracing morphological evolution of galaxies through cosmic time

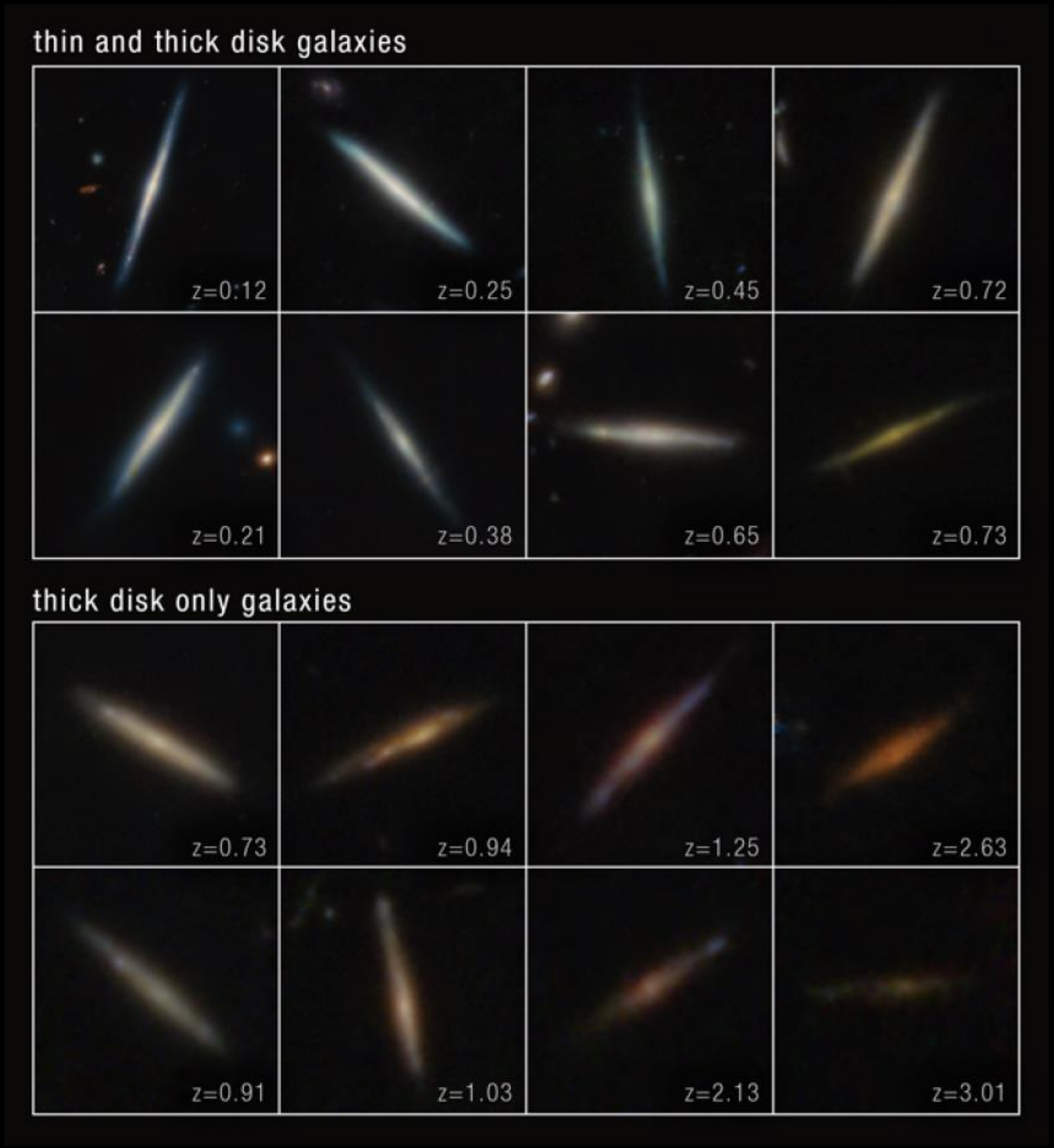

See also Lian & Luo+24

Galaxies at high$-z$

- Disc substructures (like bar and spiral) already appeared at the early time of the Universe
- Tracing morphological evolution of galaxies through cosmic time
- Link Milky Way to the morphological evolution of high-z galaxies
- What is the evolutionary pathway of the Milky Way's disc

@ESA/Gaia/DPAC

How do stars move after they formed?

Secular evolution in the Galactic disc

- Orbits of stars do not remain constant

- Stars could move from their birth radius to their present-day radius, called radial migration

- This process happens through interaction with non-axisymmetric perturbations, e.g. the transient spiral arms, galactic bar.

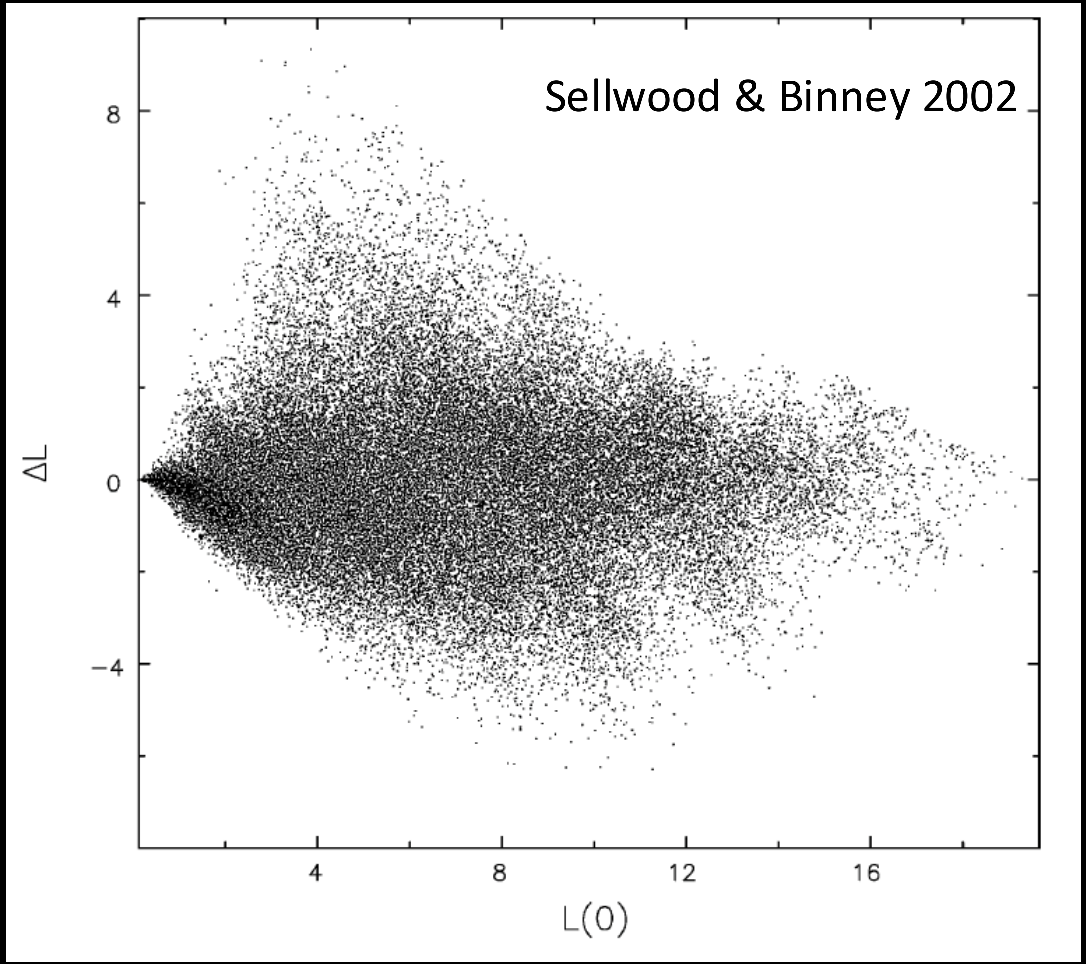

See Sellwood & Binney 02, Minchev & Famaey 10, Halle+15, Khoperskov+20, Haywood+24, Marques+25 (etc…) for different radial migration mechanisms

Secular evolution in the Galactic disc

Credit: Neige Frankel

- Orbits of stars do not remain constant
- Stars could move from their birth radius to their present-day radius, called radial migration
- This process happens through interaction with non-axisymmetric perturbations, e.g. the transient spiral arms, galactic bar.

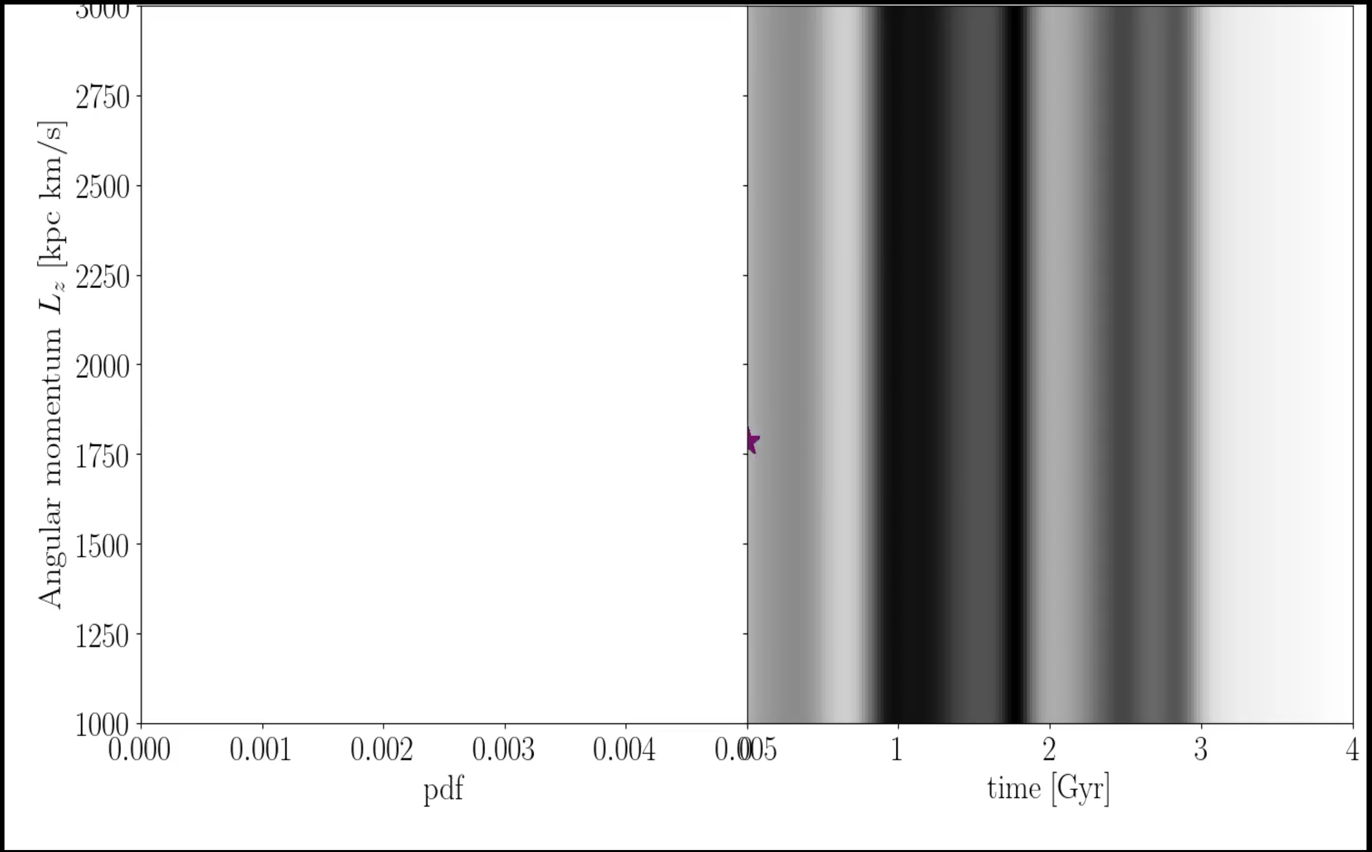

See Sellwood & Binney 02, Minchev & Famaey 10, Halle+15, Khoperskov+20, Haywood+24, Marques+25 (etc…) for different radial migration mechanisms

Signatures of radial migration

- As the Galactic ISM are axisymmetric within ≲0.1 dex (Wenger+19, etc.), the observed stellar metallicity in the solar neighbourhood should have little spread at each ages.

- The large metallicity spread in the stellar metallicity at each age reflects the amount of radial migration in the Galactic disc.

$$\sigma_{L_z} \sim \frac{V_c\, \sigma_{[\mathrm{Fe/H}]}}{|d[\mathrm{Fe/H}]/dR|}$$

See Sellwood & Binney 02, Frankel+20, Ratcliffe+25

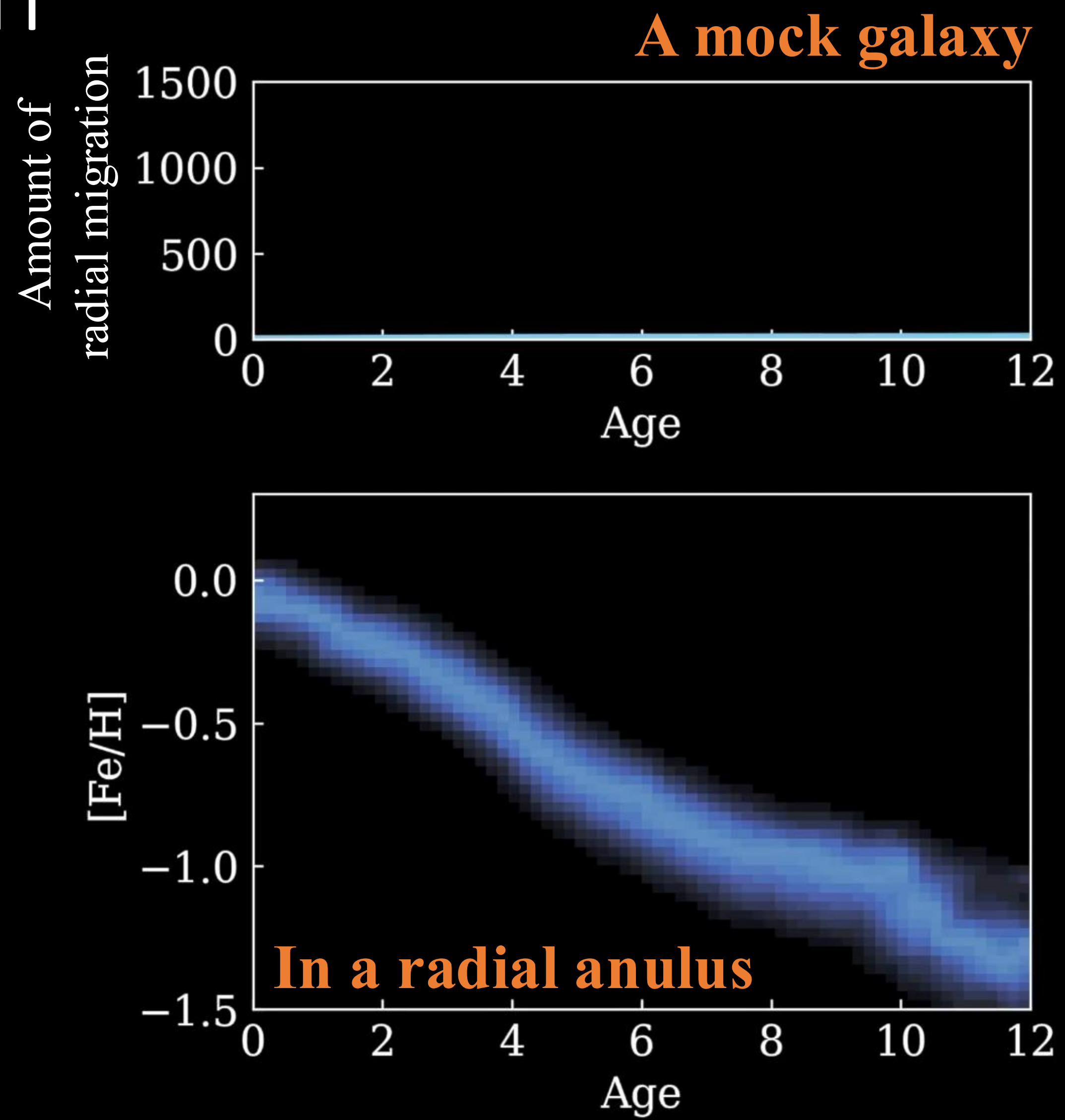

Signatures of radial migration

- As the Galactic ISM are axisymmetric within $\lesssim$0.1 dex (Wenger+19, etc.), the observed stellar metallicity in the solar neighbourhood should have little spread at each ages.

- The large metallicity spread in the stellar metallicity at each age reflects the amount of radial migration in the Galactic disc.

$$\sigma_{L_z} \sim \frac{V_c \, \sigma_{[\mathrm{Fe/H}]}}{|d[\mathrm{Fe/H}]/dR|}$$

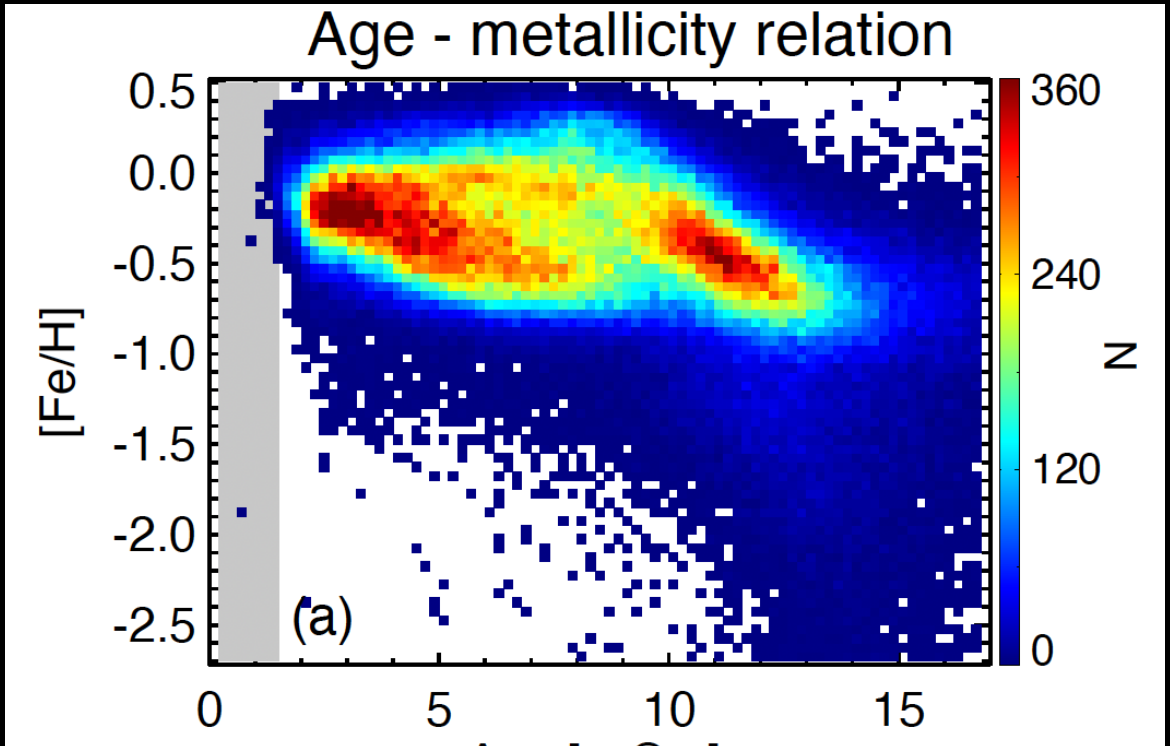

Xiang & Rix 2022

See Sellwood & Binney 02, Frankel+20, Ratcliffe+25

One way of solving this: birth radius inference

- Can estimate birth radii R_b of stars from stellar ages and metallicity: $\{\tau, [\mathrm{Fe/H}]\} \rightarrow R_b$
- ISM metallicity model $[\mathrm{Fe/H}](R_b, \tau)$
  $[\mathrm{Fe/H}](R_b, \tau) = [\mathrm{Fe/H}]_0(\tau) + \nabla[\mathrm{Fe/H}]R_b$
    1) maximum metallicity at each age
    2) metallicity spread at each age
- One can then comparing R_{today} and R_b to map the secular evolution

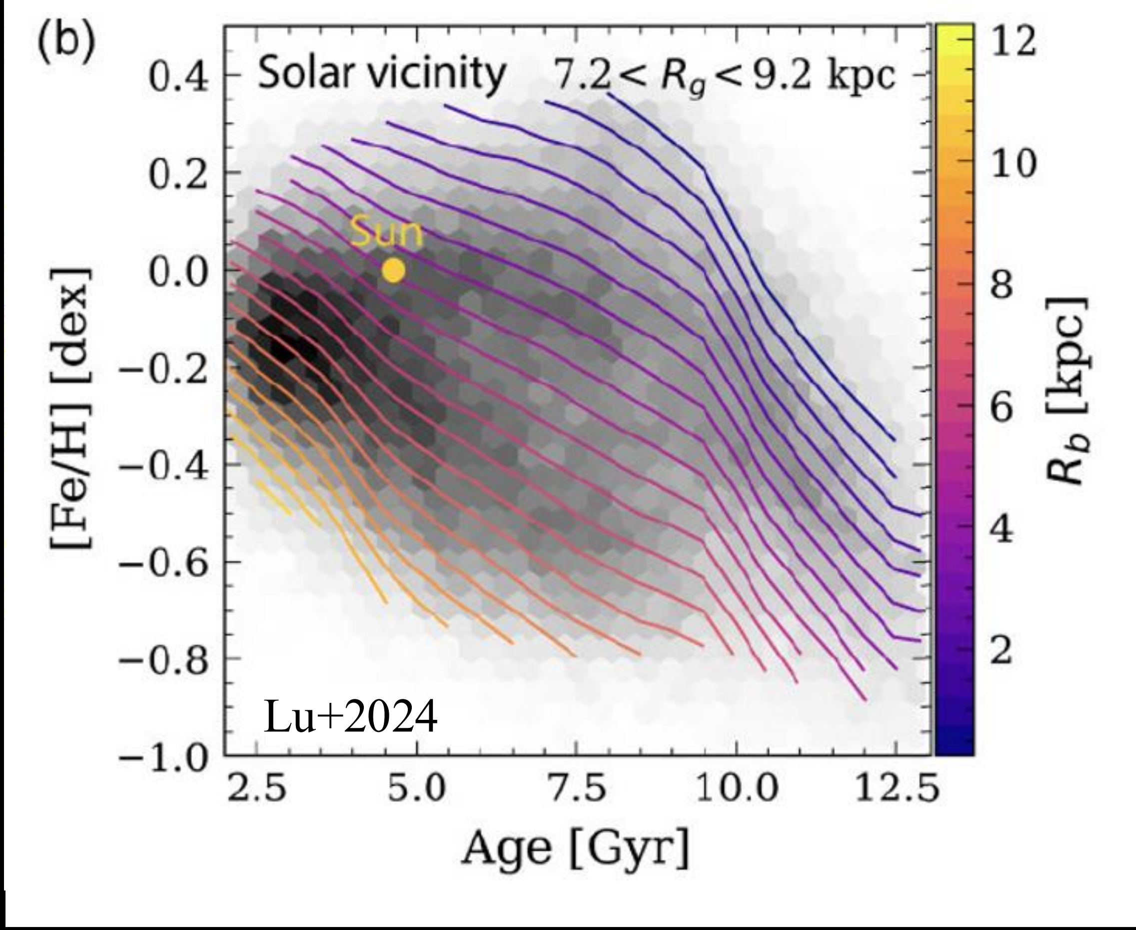

See Minchev+2018, Lu+2024, Ratcliffe+2024

LAMOST: Age vs [Fe/H] vs R_g

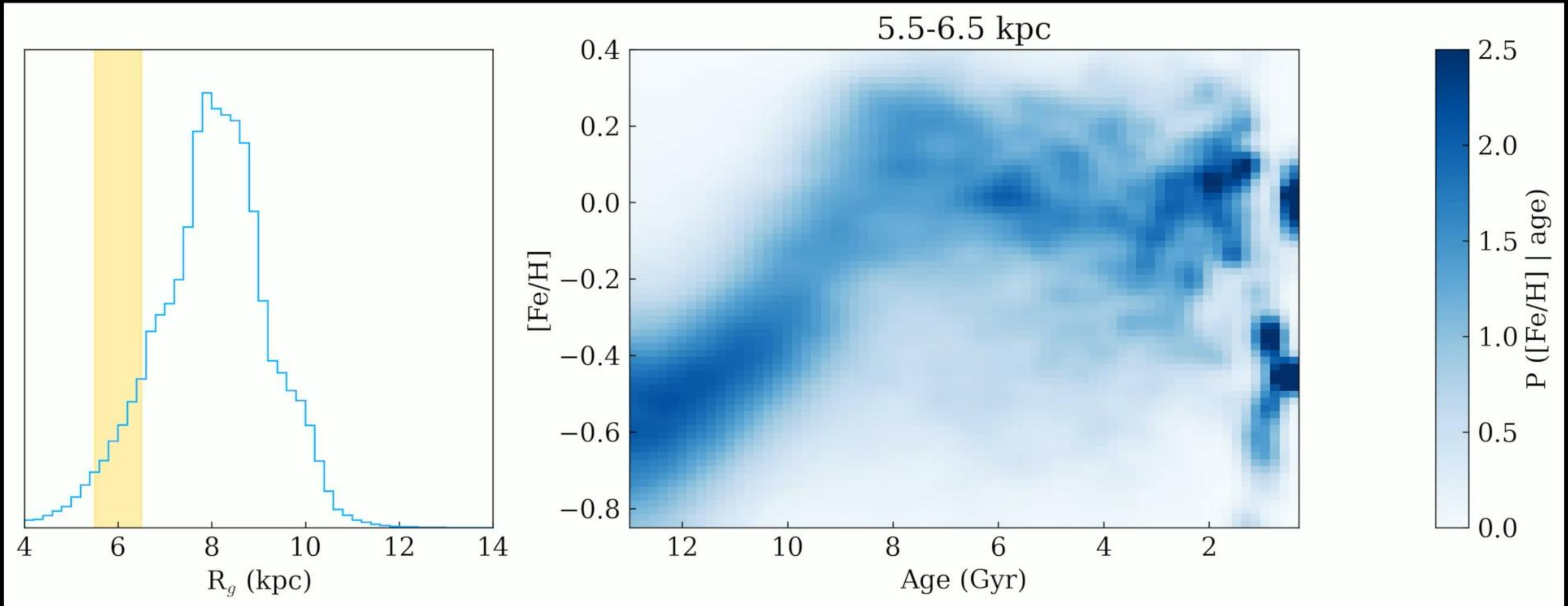

Isochronal ages from Xiang et al. 2025

Test-particle simulation: bar-driven migration

Initialise a quasi-isothermal disc in an axisymmetric disc potential

Grow a galactic bar in the background potential with an initial pattern speed $\Omega_i = 80$ km/s/kpc ($R_{CR,init} \sim 3$ kpc)

Bar reach its maximum strength and start decelerate with $\eta = -\dot{\Omega}/\Omega^2 = 0.003$

Final pattern speed $\Omega_0 = 34$ km/s/kpc ($R_{CR,0} \sim 7$ kpc)

t = 0 Gyr | t = 3.5 Gyr | t = 4.5 Gyr | t =11.5 Gyr

Add new disc stellar particles into the simulation constantly with time

Assign metallicity to the test particles afterwards with a model [Fe/H] $= f(R_b, \tau)$

Cut $d_{Sun} < 3$ kpc to mimic the coverage of the subgiant sample

HZ et al. 2025a

Resulting age-metallicity sequences

Local stars vs. migrated stars

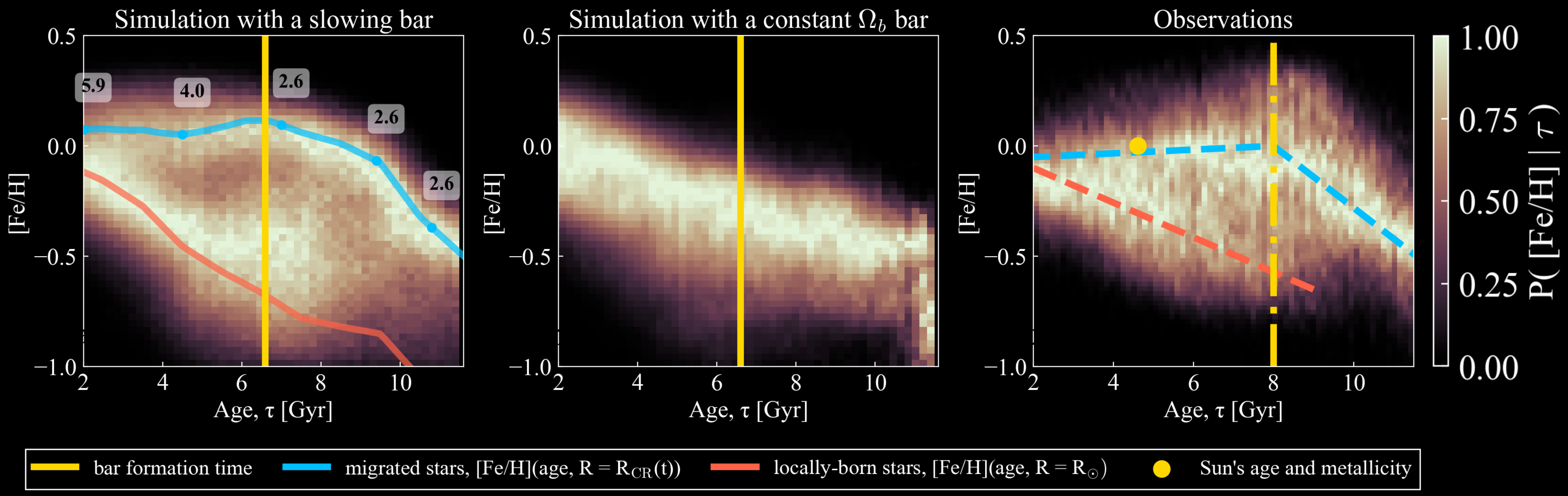

HZ+2025a

Resonant dragging of a decelerating bar

A toy demonstration

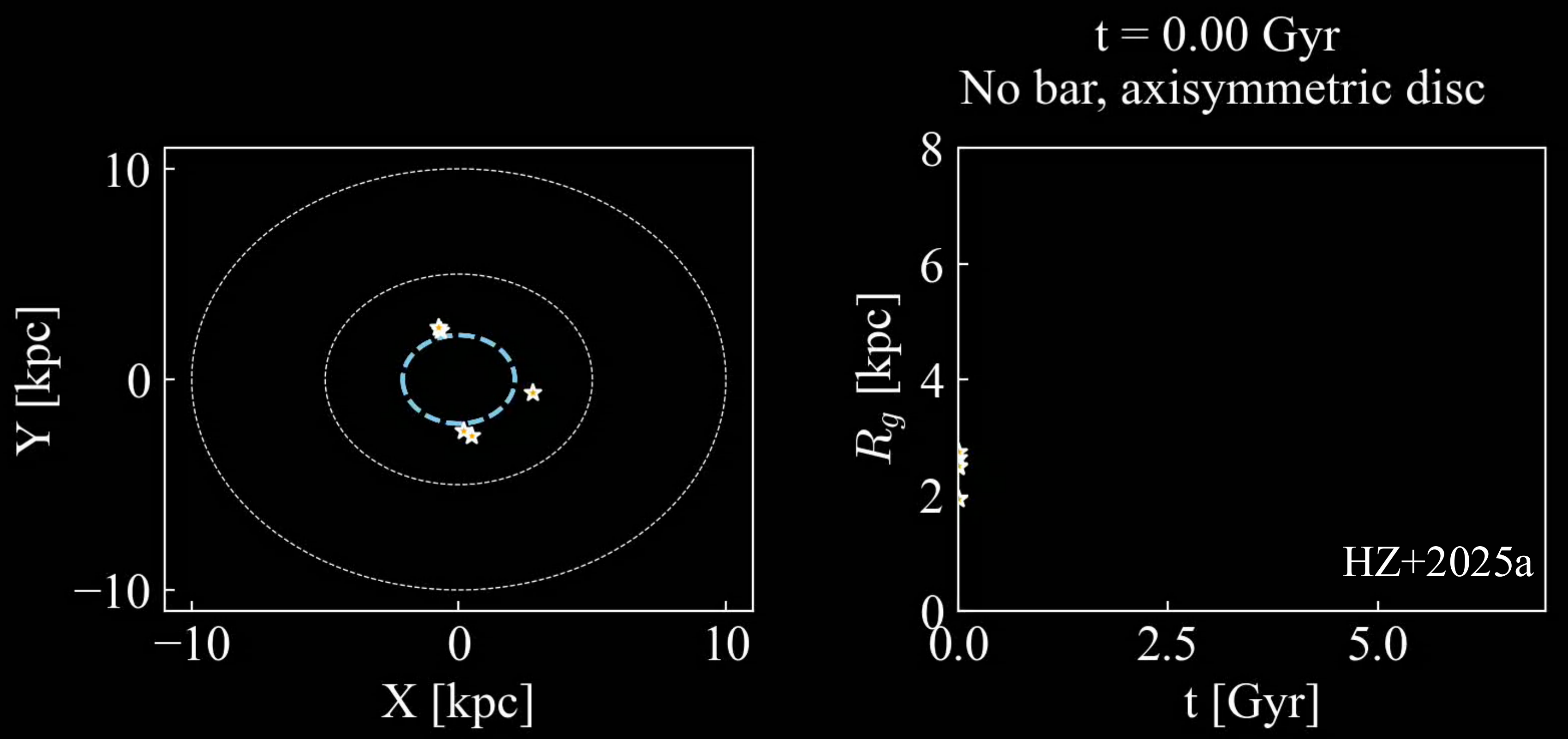

Stars trapped in the corotation resonance migrate with the expansion of the corotation. This brings stars from the inner Milky Way to the present-day corotation radius.

See Chiba+21; Chiba & Schonrich 2021 for analytic descriptions

Today's pattern speed ~ 32 − 34 km/s/kpc (Chiba+21, Clarke+22, **HZ**+24, Dillamore+25); corotation radius ~ 7 − 7.5 kpc

Resulting age-metallicity sequences

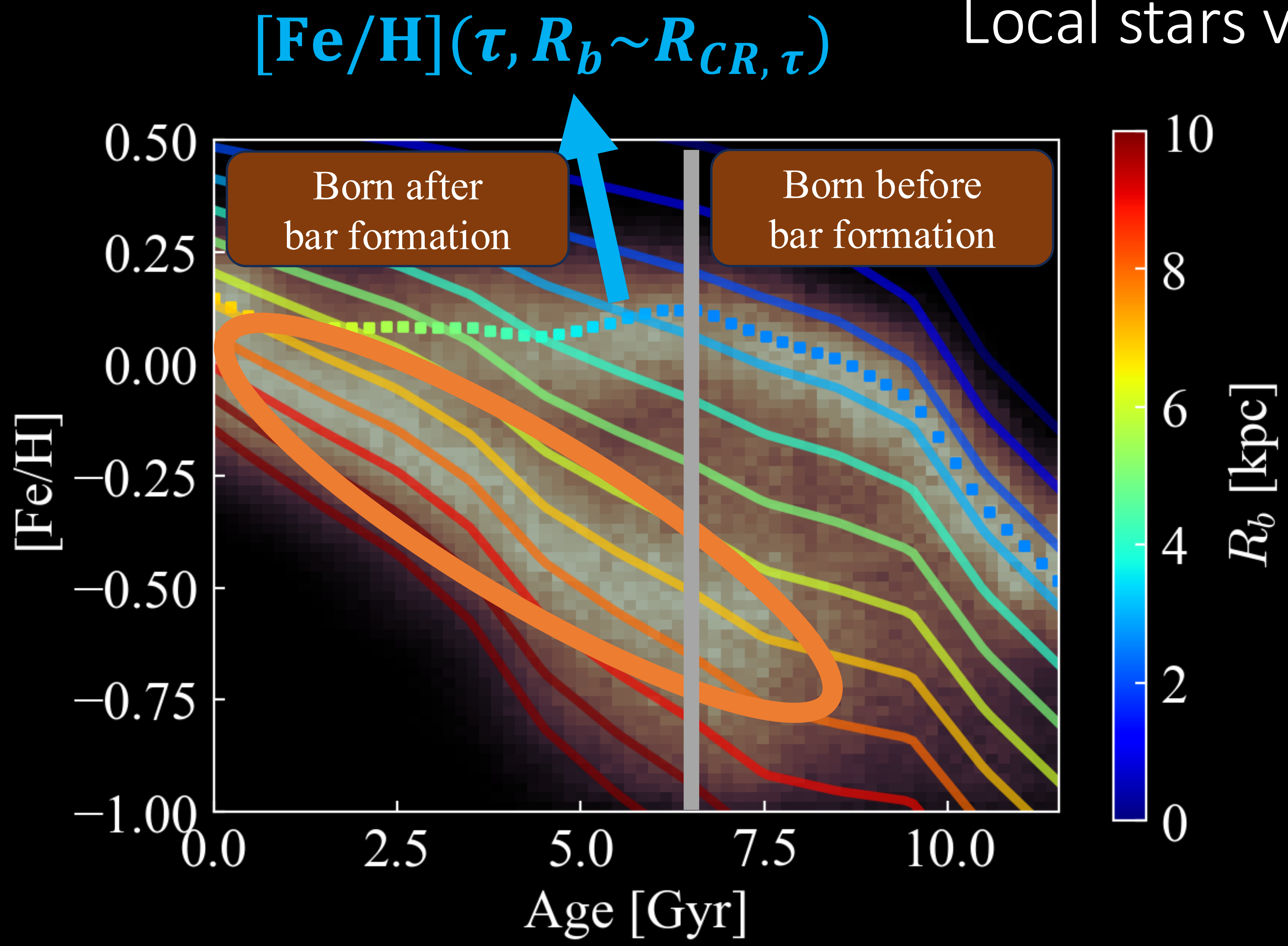

Local stars vs. migrated stars

Stars born ***before bar formation***: those that has $R_b \sim R_{CR,\,init}$ experience strong resonance dragging

Age-metallicity sequence tracks $[Fe/H](\tau, R_b \sim R_{CR,\,init})$

Stars born ***after bar formation:*** those that has $R_b \sim R_{CR}(t = \tau)$ experience strong resonance dragging

Age-metallicity sequence flattens, and tracks $[Fe/H](\tau, R_b \sim R_{CR,\,\tau})$

Resulting age-metallicity sequences

The guiding radii dependence

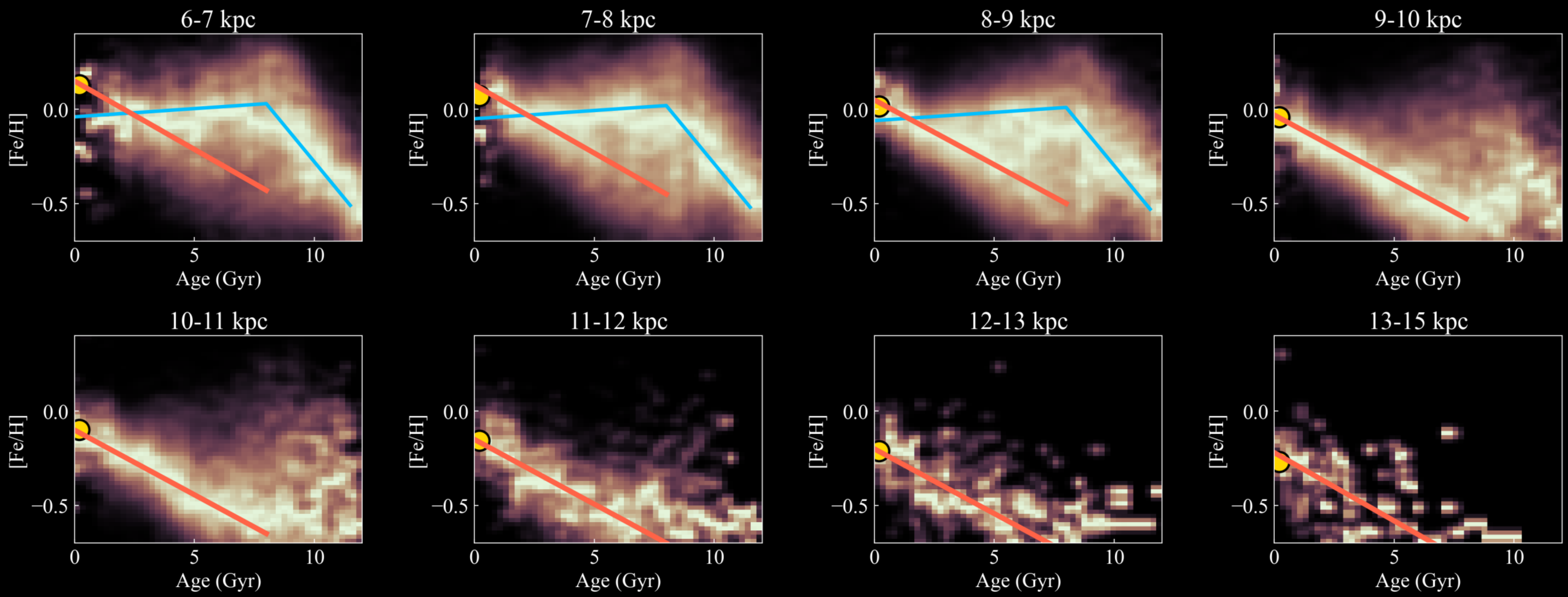

● = gas-phase metallicity today

Resulting age-metallicity sequences

The guiding radii dependence

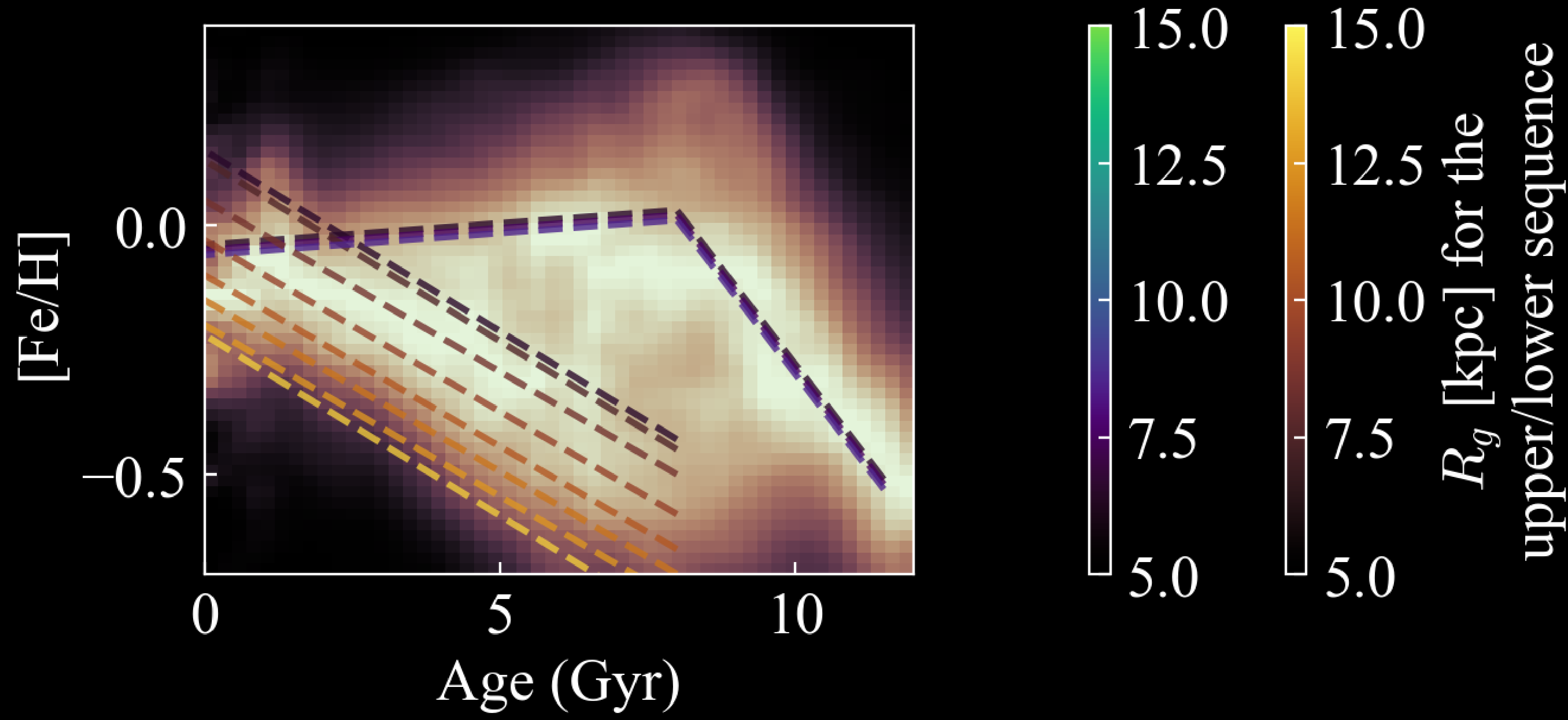

See also Khoperskov+25

Implications: $[\alpha/\mathrm{Fe}] - [\mathrm{Fe/H}]$ bimodality

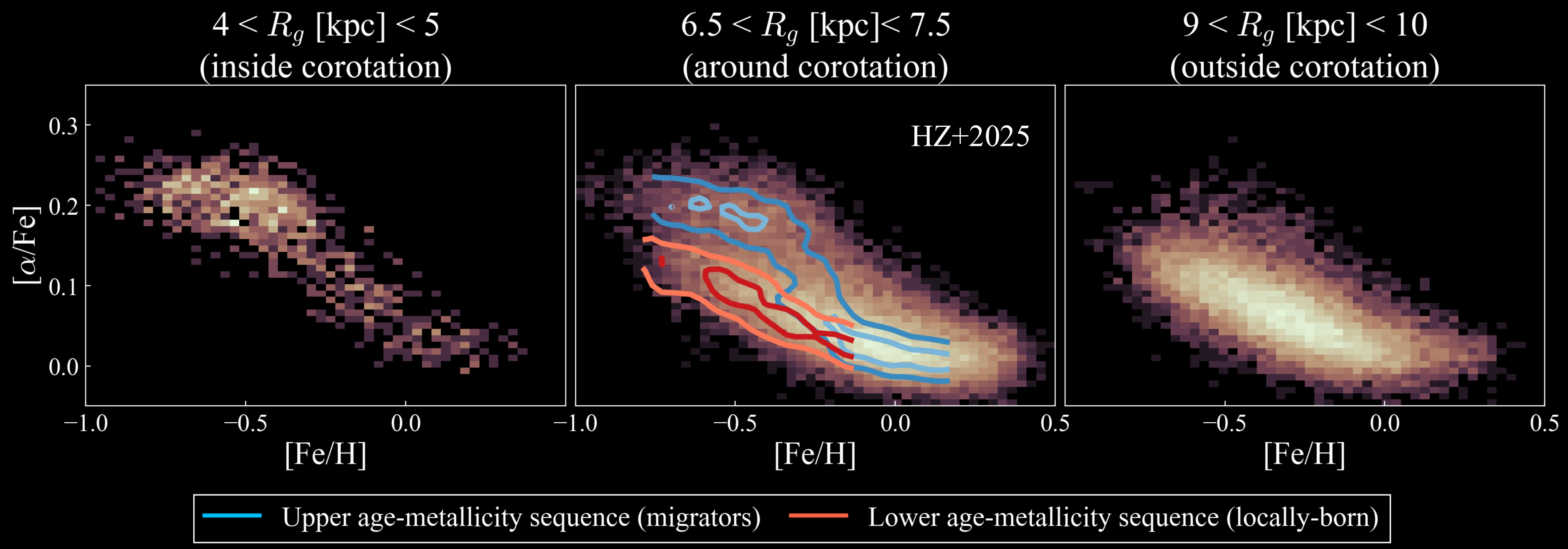

See more detailed chemical cartography map in Hayden+15

See also Sharma+21

Inferring the pattern speed history of the bar

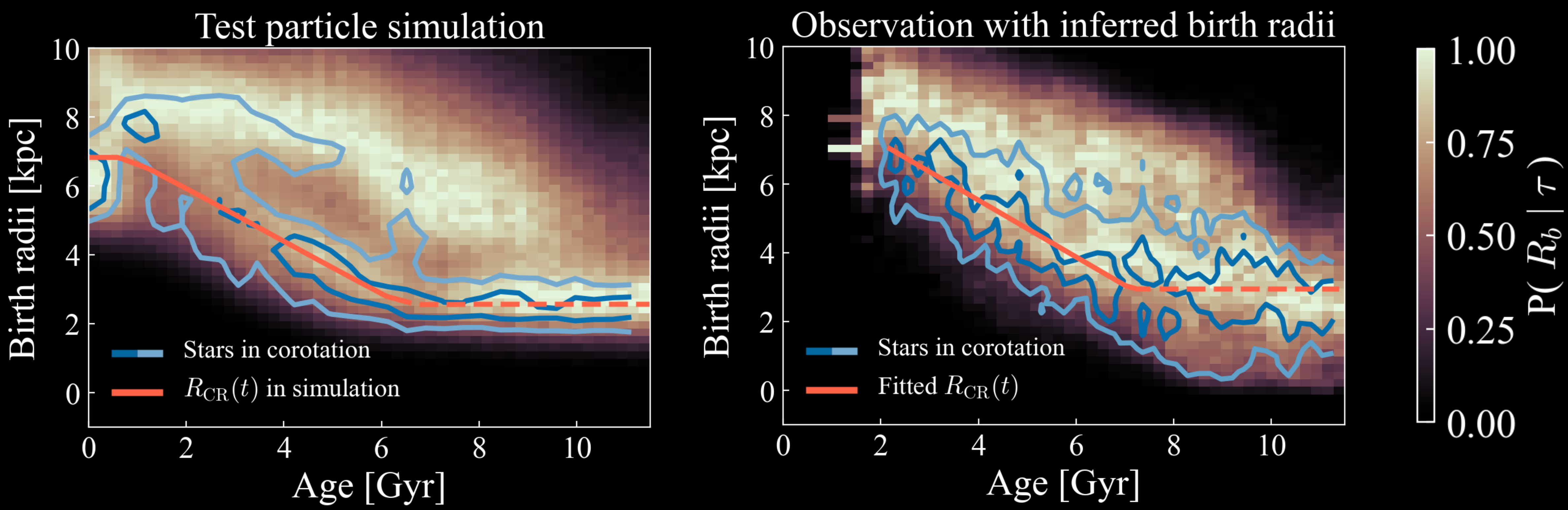

In this birth radius calculation method (Lu+24), we can infer:

$$t_{bf} \sim 6 - 8 \text{ Gyr}; \Omega_i \sim 60 - 80 \text{ km/s/kpc}; \eta = -\dot{\Omega}/\Omega^2 \sim 0.0025 - 0.004$$

agree with other independent measurements of t_{bf} and η (Chiba+21, Sanders+24), and non-independently Haywood+24

Half-time break

- Corotation resonance of decelerating bar can create the V-shaped age-metallicity pattern
- Can be used to explain the α-bimodality of the disc
- Can infer the history of bar deceleration (e.g. formation time, initial pattern speed and deceleration rate) using this signature.

Next: A more comprehensive chemodynamical forward modelling approach

Chemo-chrono-dynamical modelling

- Fitting for the column-normalised age-metallicity plane at different radial bins

$$p\left([\mathrm{Fe/H}]\middle|\tau, R_g\right) = \frac{p([\mathrm{Fe/H}], R_g|\tau)}{\int d[\mathrm{Fe/H}]\, p([\mathrm{Fe/H}], R_g|\tau)}$$

where $p\left([\mathrm{Fe/H}], R_\mathrm{g}\middle|\tau\right) =$

$$\int dL_{z,b} \left\{ p\left([\mathrm{Fe/H}]\middle|\tau, L_{z,b}\right) p\left(L_{z,b}\middle|\tau\right) p\left(L_z\middle|\tau, L_{z,b}\right) \right\}$$

Stellar metallicity at birth (ISM metallicity)

Initial radial profile

Radial migration kernel

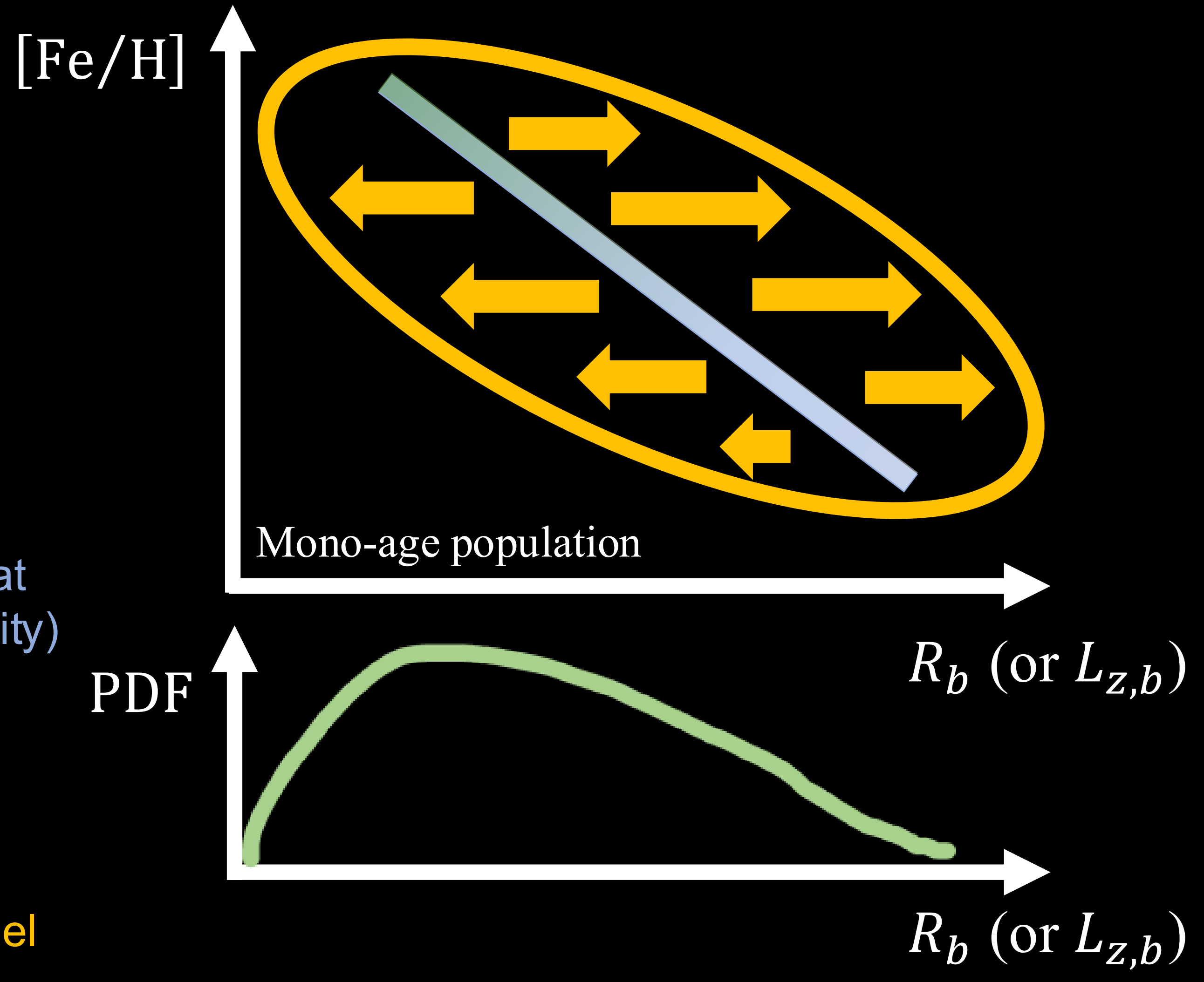

HZ+2025b

See also similar models in Frankel+18, 20

Chemo-chrono-dynamical modelling

With observables: $\{\tau, [Fe/H], x, y, z, v_x, v_y, v_z\}$

Disc growth

$$p(L_{z,b}|\tau) \propto L_{z,b} \exp[-\frac{L_{z,b}}{V_{circ}R_{d,0}}]$$

$\rightarrow$ $R_{d,0}(\tau)$

Initial disc scale length (Star-forming disc scale length)

Weak chemical tagging

$$\overline{[\mathrm{Fe/H}]}_{\mathrm{ISM}} = [\mathrm{Fe/H}]_0 + \nabla[\mathrm{Fe/H}]\ R_b$$

$\rightarrow$ $\nabla[\mathrm{Fe/H}](\tau)$ (ISM)

Radial metallicity gradient at birth (Gas-phase metallicity gradient)

Orbital diffusion

$$p(L_z|L_{z,0},\tau) = \mathcal{N}\left(L_z \,\middle|\, L_{z,b} - \frac{\sigma_{Lz}^2}{2V_{circ}R_{d,0}}, \sigma_{Lz}\right)$$

$$p(v_R, v_z|R, R_g, z) \propto \exp[\frac{-J_R\kappa}{\sigma_R^2}]\exp[\frac{-J_z\nu}{\sigma_z^2}]$$

$\rightarrow$ $\sigma_{L_z}(\tau, R_g)$, $\sigma_R(\tau, R_g)$, $\sigma_z(\tau, R_g)$

Angular momentum diffusion coefficient

+

Radial and vertical velocity dispersion

Validation against selection function & uncertainties

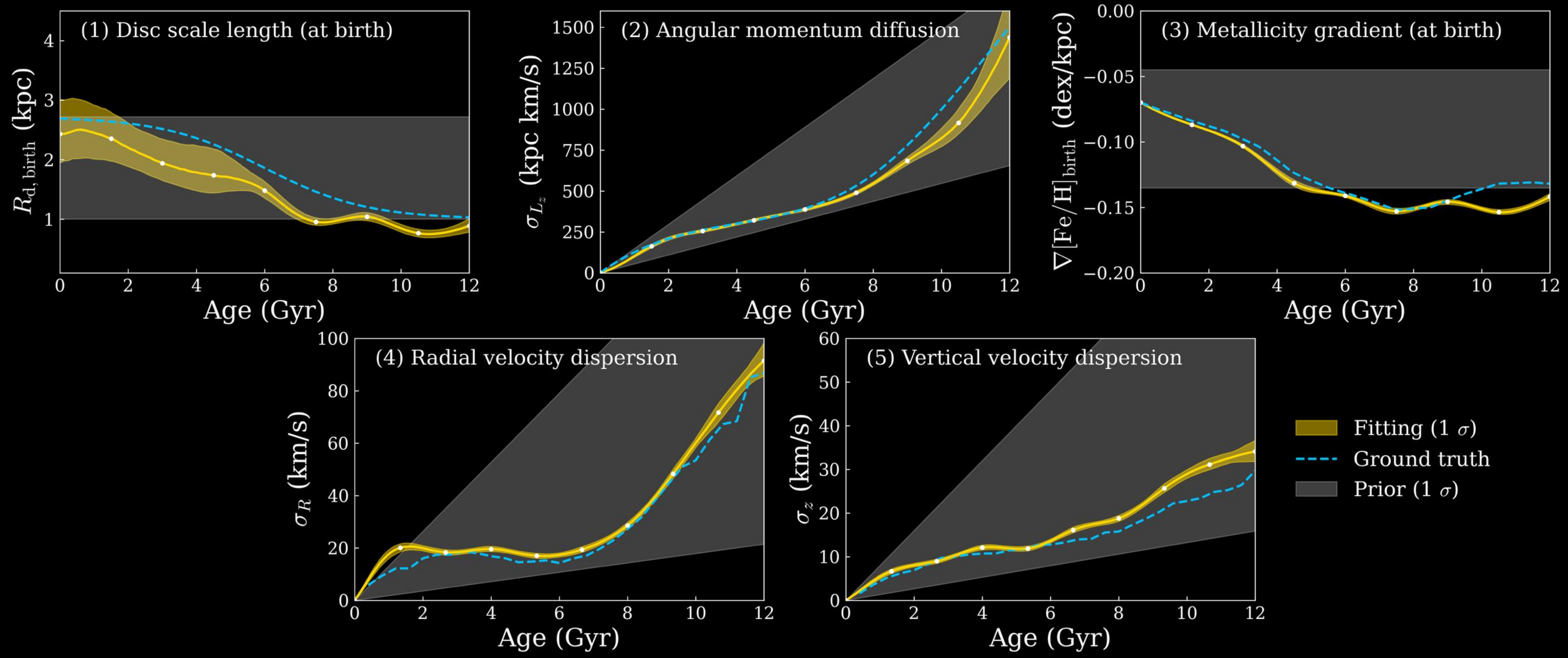

HZ+2025b

Model fits to data well

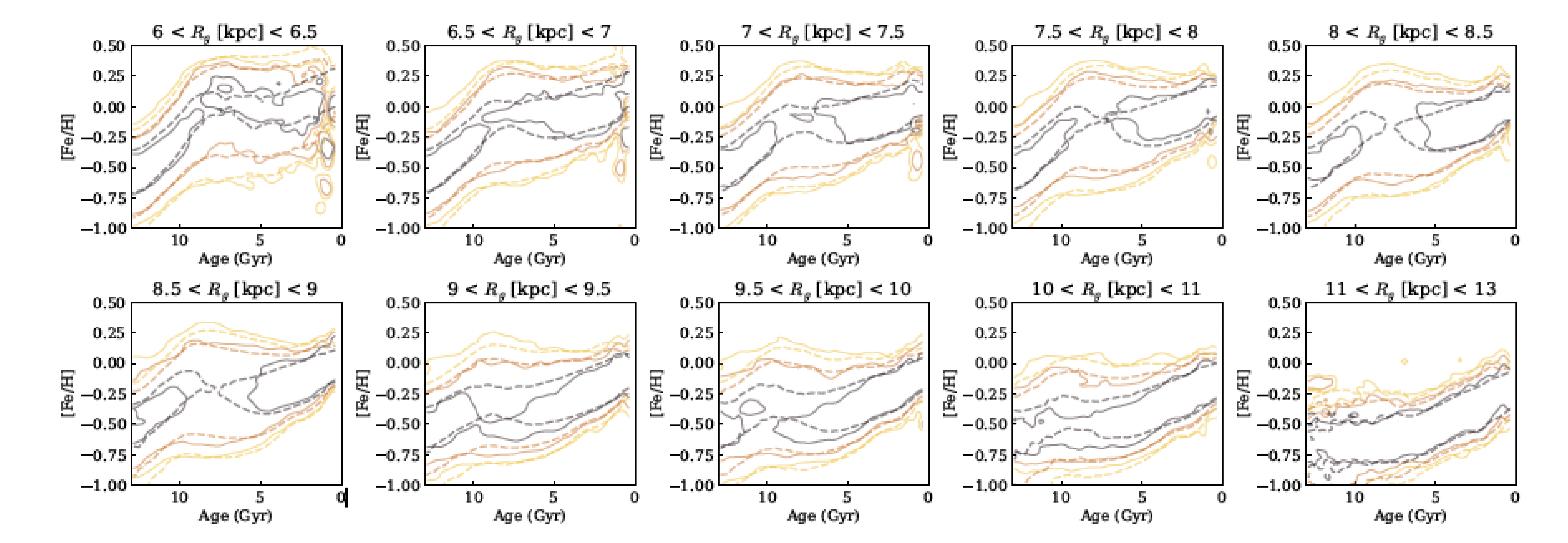

Results: Inside-out formation

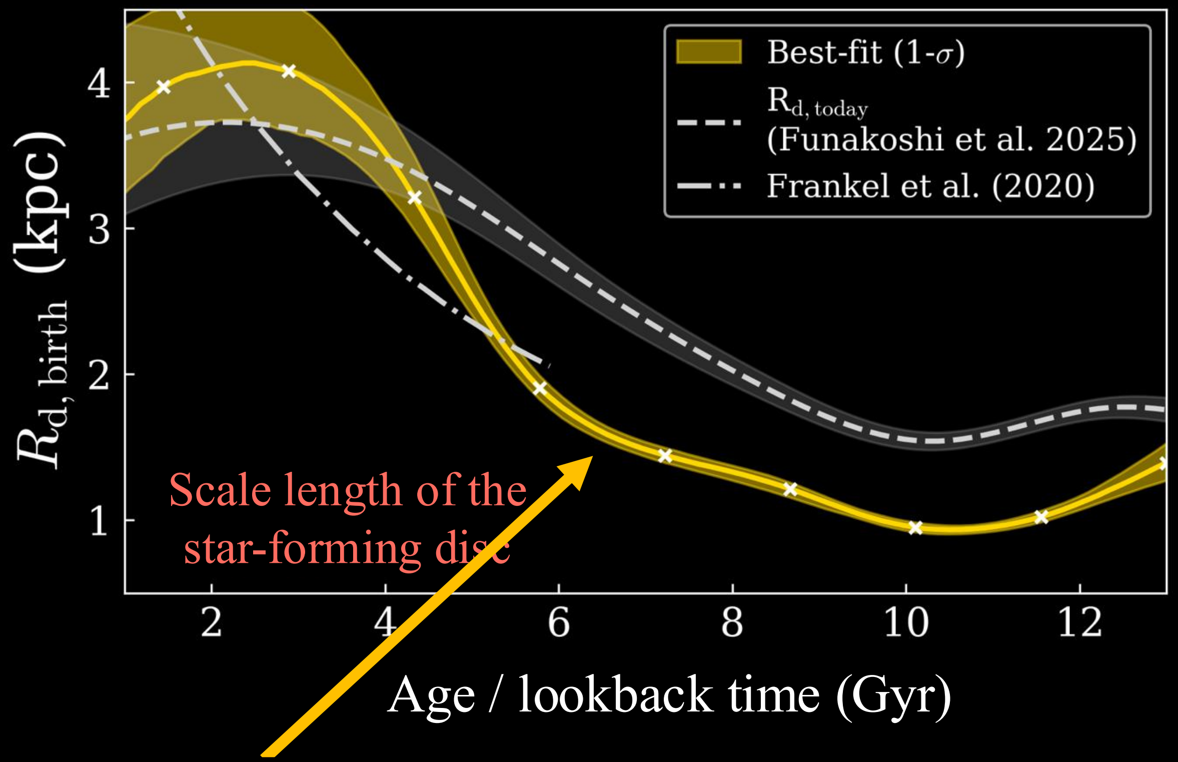

Sharp increase in the star-forming disc scale length: Gas accretion?

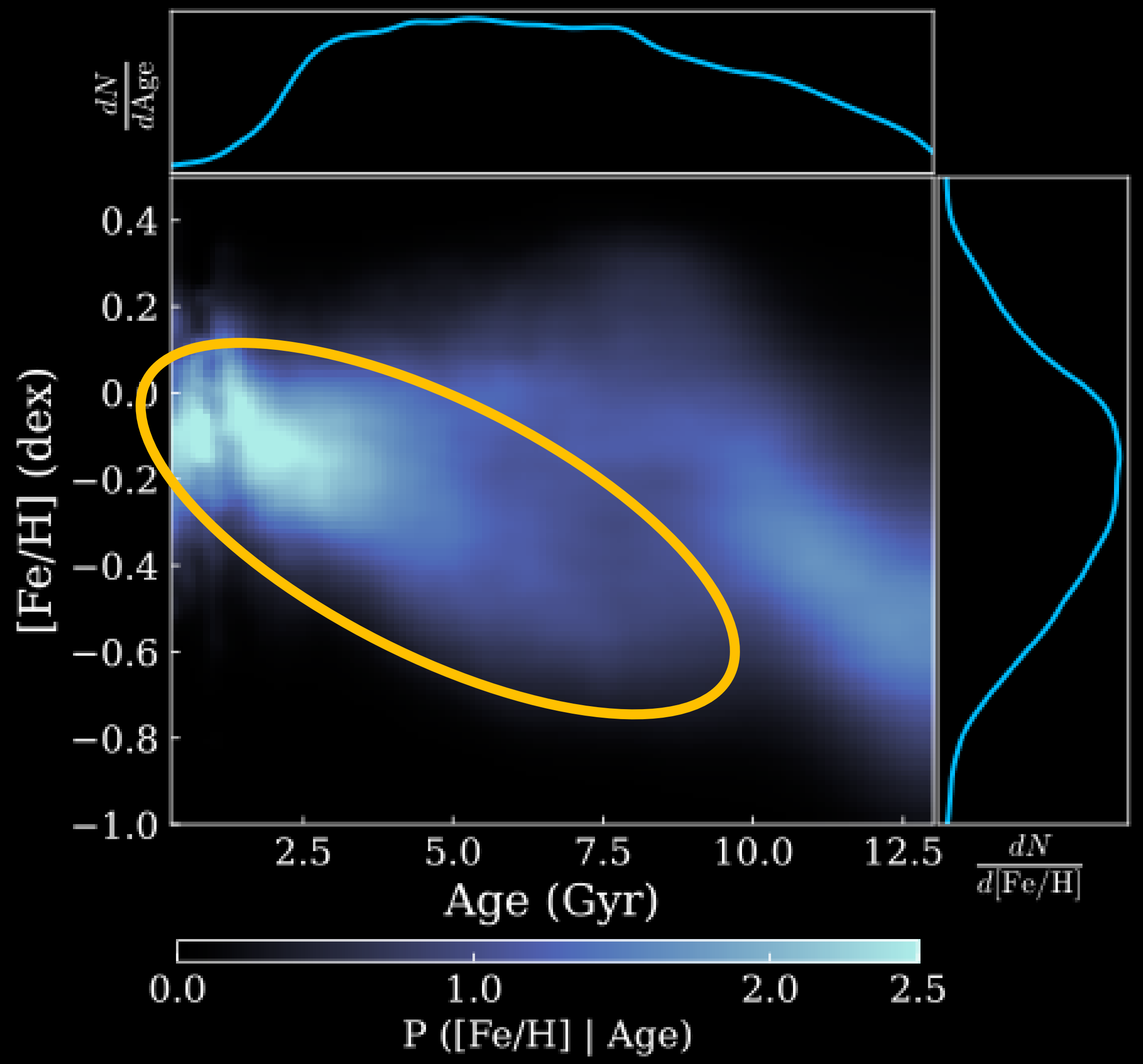

HZ+2025

See also the results in Ratcliffe+26

Results: metallicity gradient

See similar results in Lu+24, Ratcliffe+25

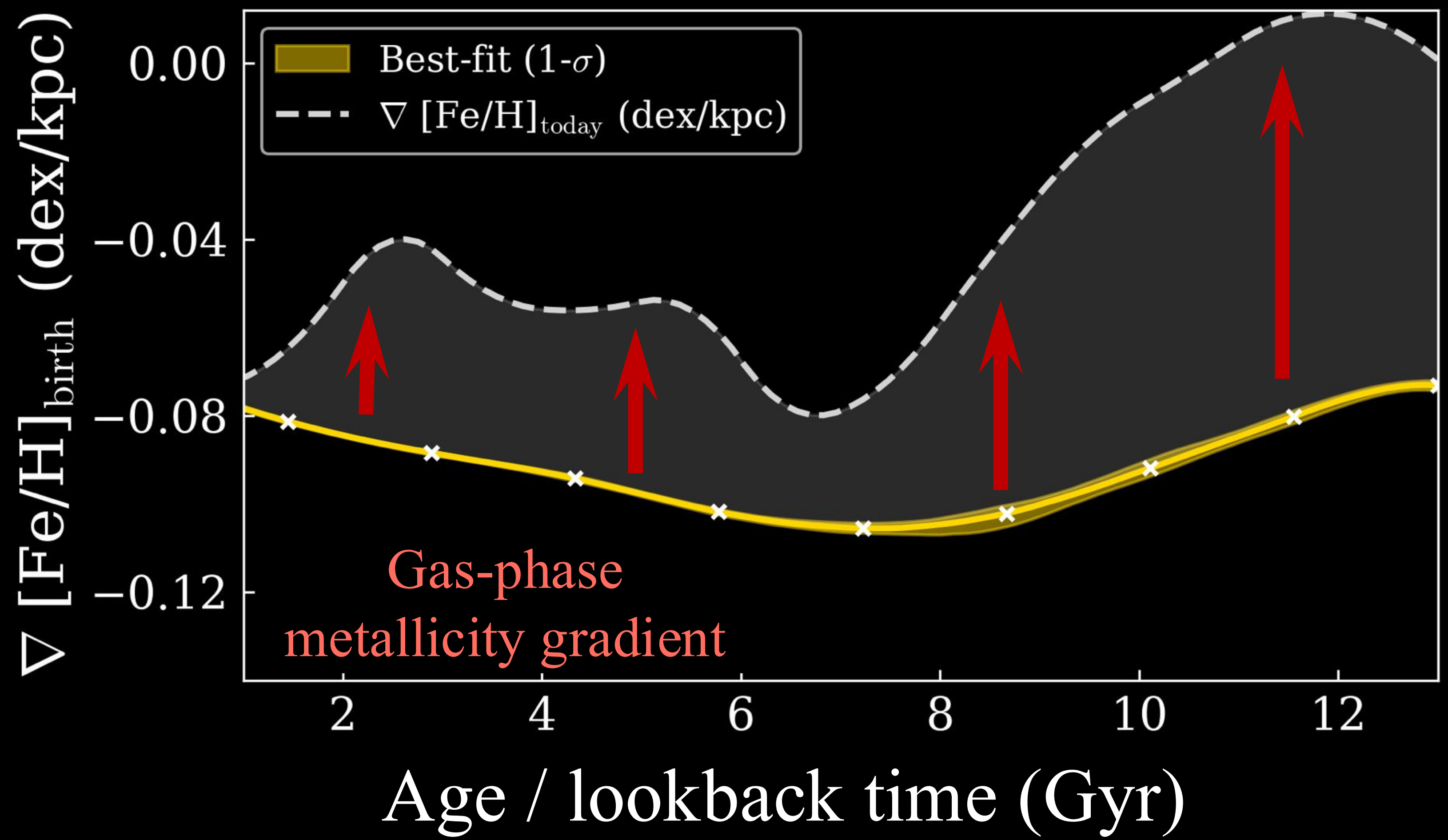

An approximately flat but constantly negative birth metallicity gradient since the disc formation

HZ+2025

Radial migration strength

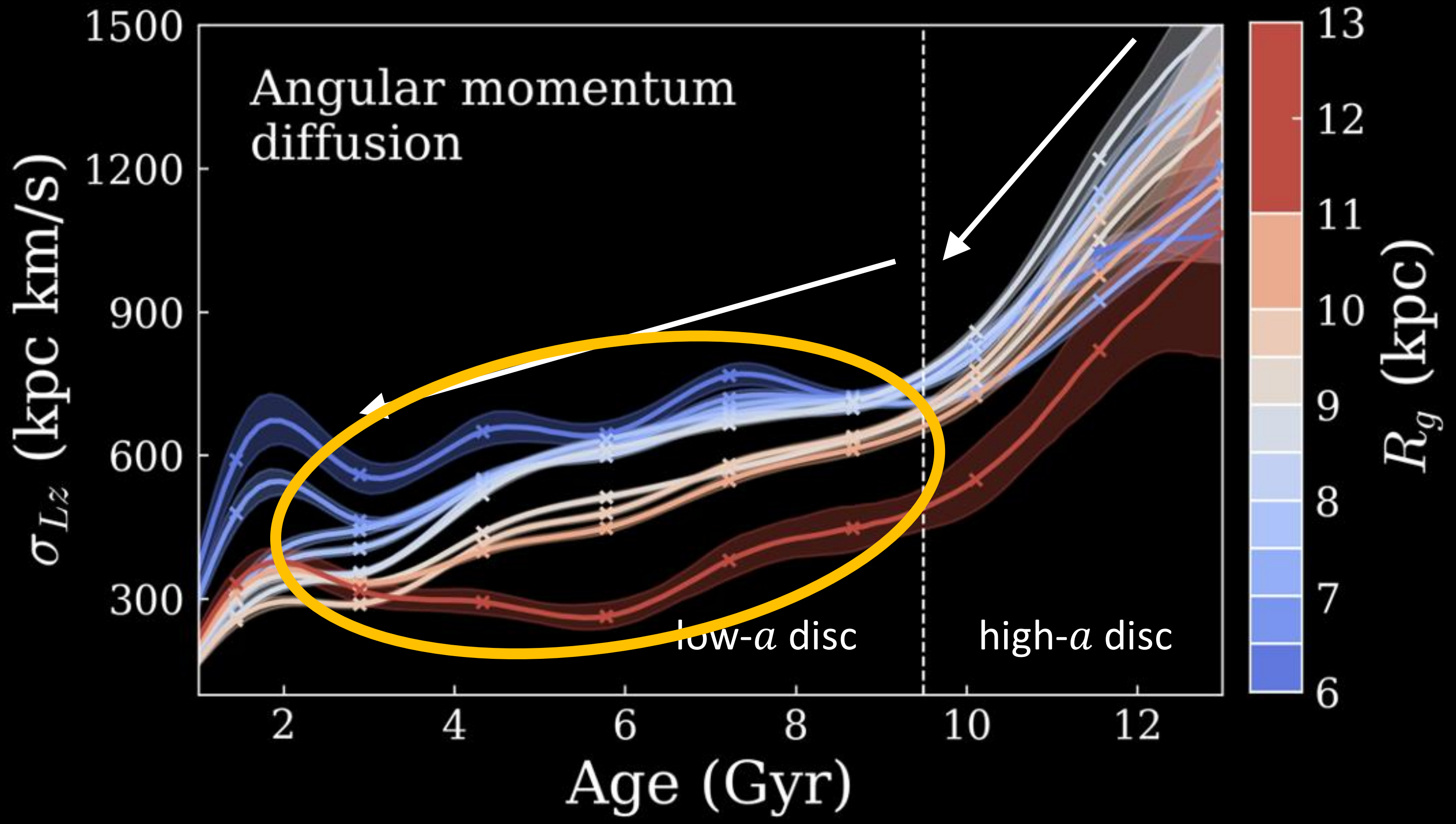

- High angular momentum diffusion in the old, high-α disc compared to the young, low-α disc

- σ_{Lz} is separated into three radial bins
  1) $6.5 < R_g$ / kpc < 9
  2) $9 < R_g$ / kpc < 11
  3) $R_g > 11$ kpc

HZ+2025b

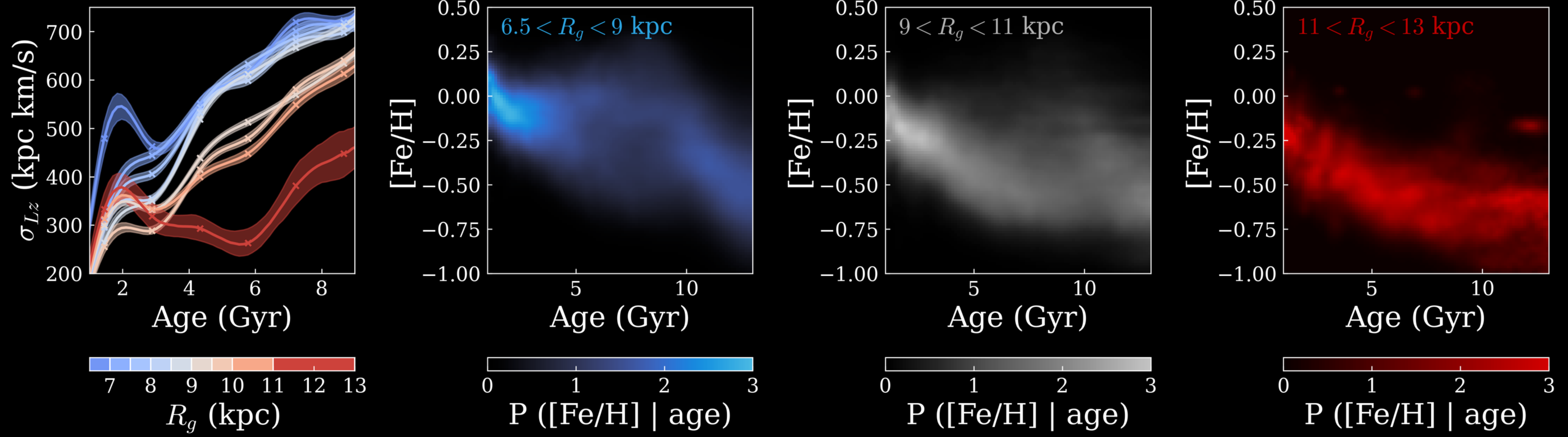

Around CR

Between CR & OLR

Outside OLR

HZ+2025b

Radial migration strength

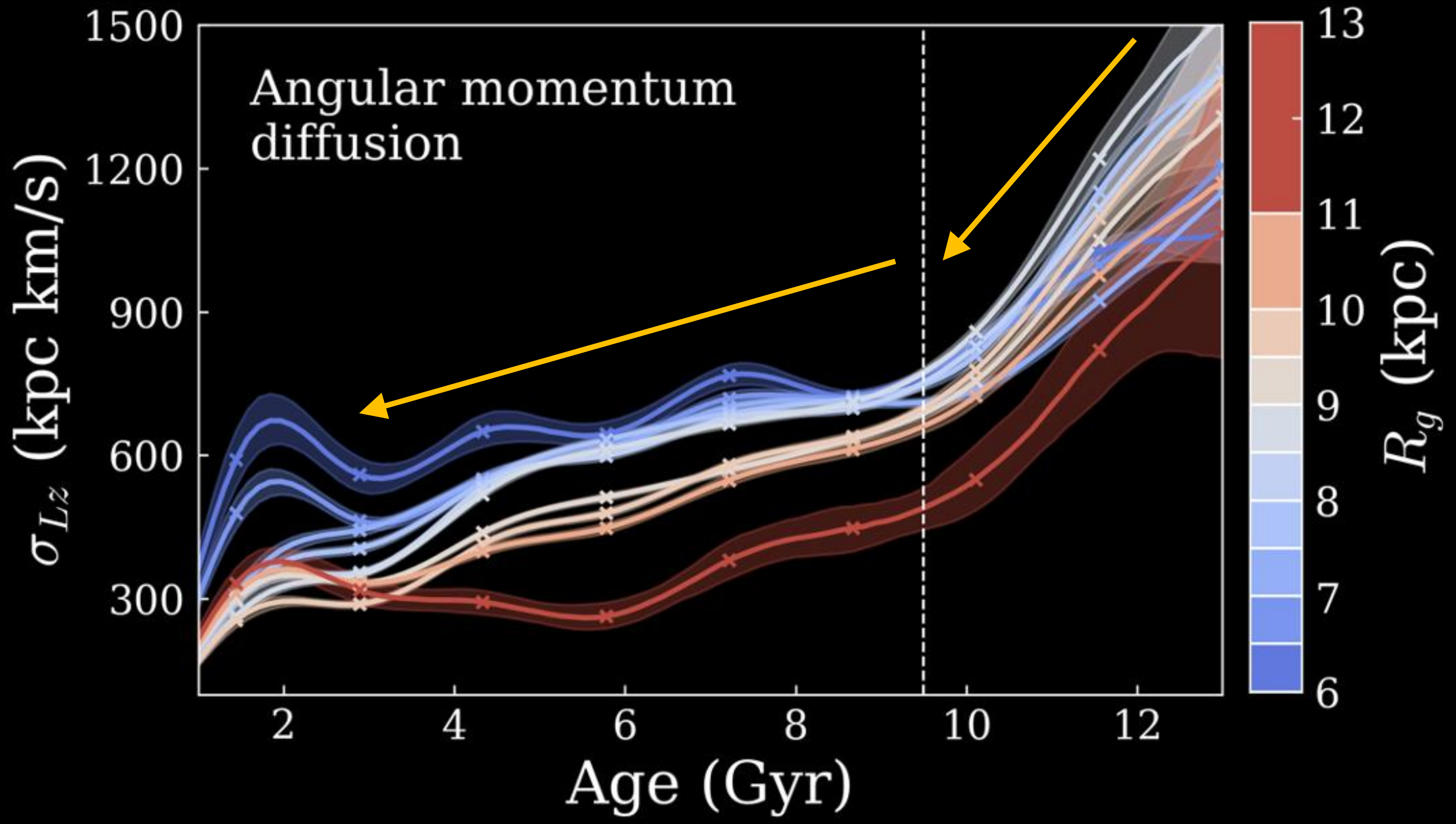

- High angular momentum diffusion in the old, high-α disc compared to the young, low-α disc

- σ_{Lz} is separated into three radial bins
  1) $6.5 < R_g/\text{kpc} < 9$
  2) $9 < R_g/\text{kpc} < 11$
  3) $R_g > 11$ kpc

HZ+2025b

Nexus simulations: the effect of gas

- Same halo and disc mass, but different gas fraction

- Simulation suite:

  Low-mass MW-analogue (V_c~140 km/s) with gas fractions 20/40/60/80%

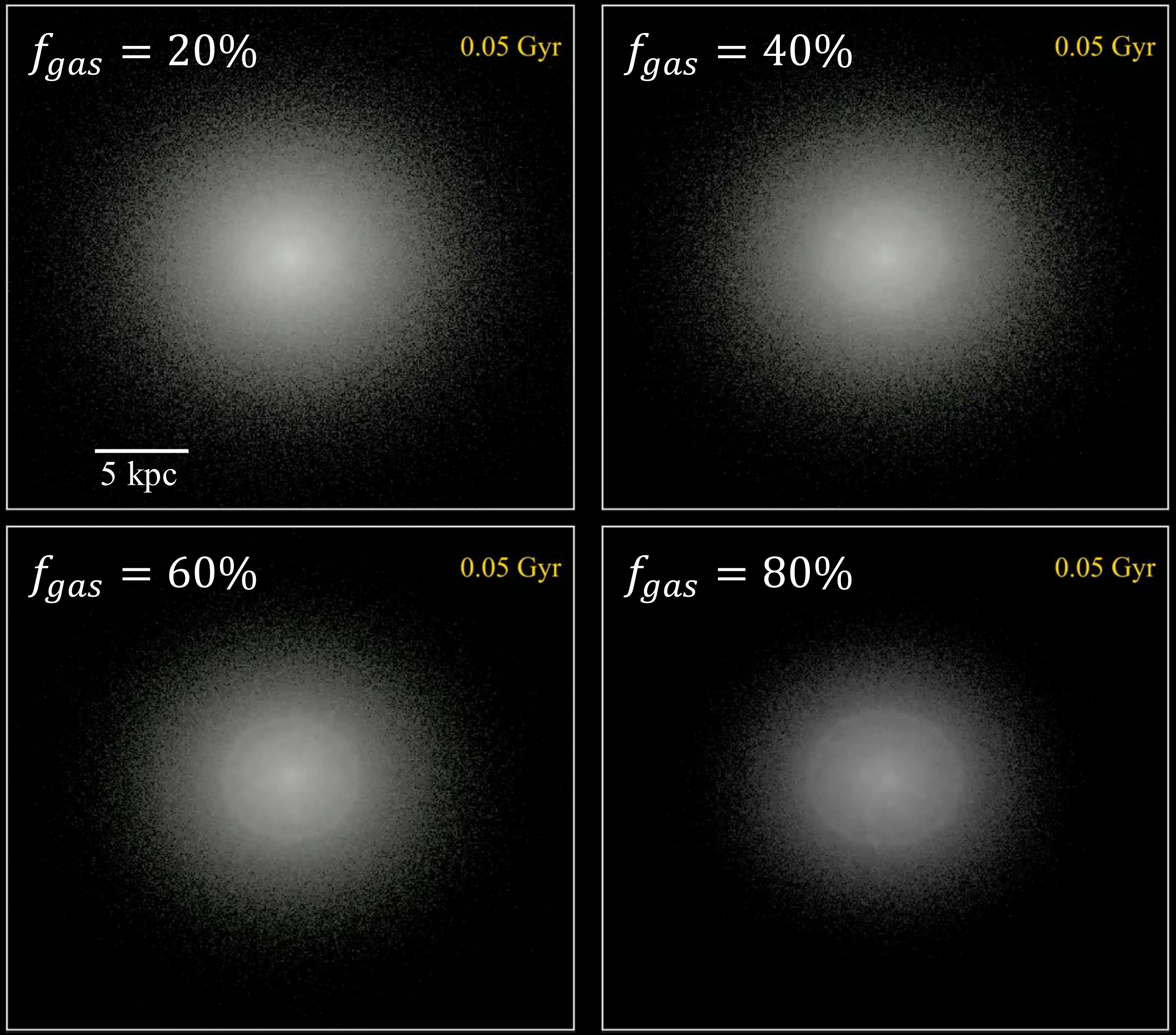

See Tepper-Garcia+2024

A quick view of the diffusion

- Computing L_z, J_R, J_z of the initial and final state of particles as orbits label
- $\delta X(t) = RMS(\Delta X) = \sqrt{\langle (X(t) - X(0))^2 \rangle}$ for $X = L_z, J_R, J_z$

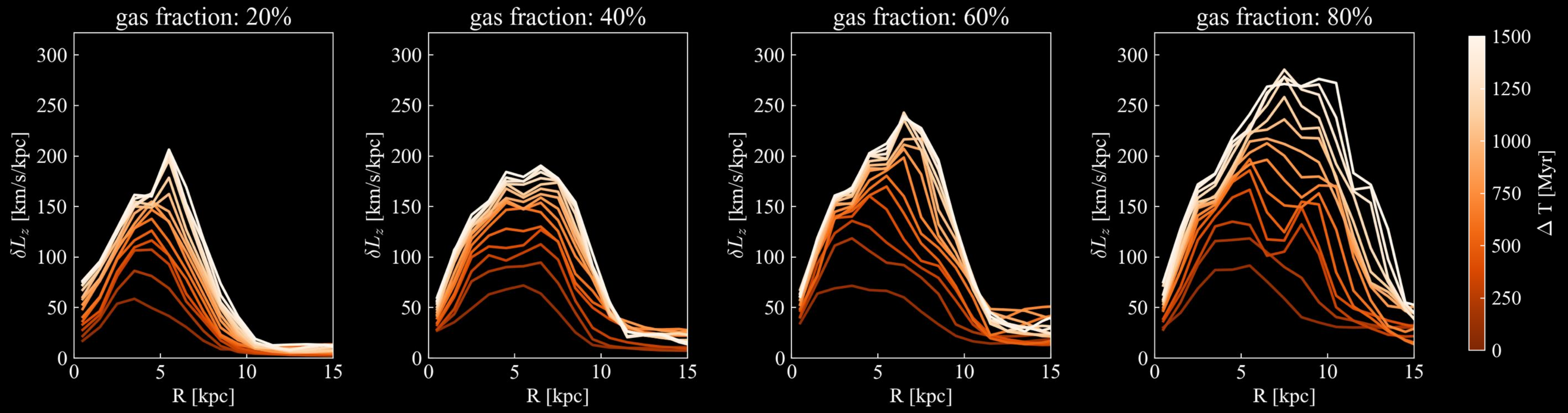

HZ+2025c

More gas = more diffusion

- More angular momentum diffusion in the more gas-rich disc
- $\delta L_z \propto \sqrt{t}$ in these isolated discs → a constant diffusion coefficient

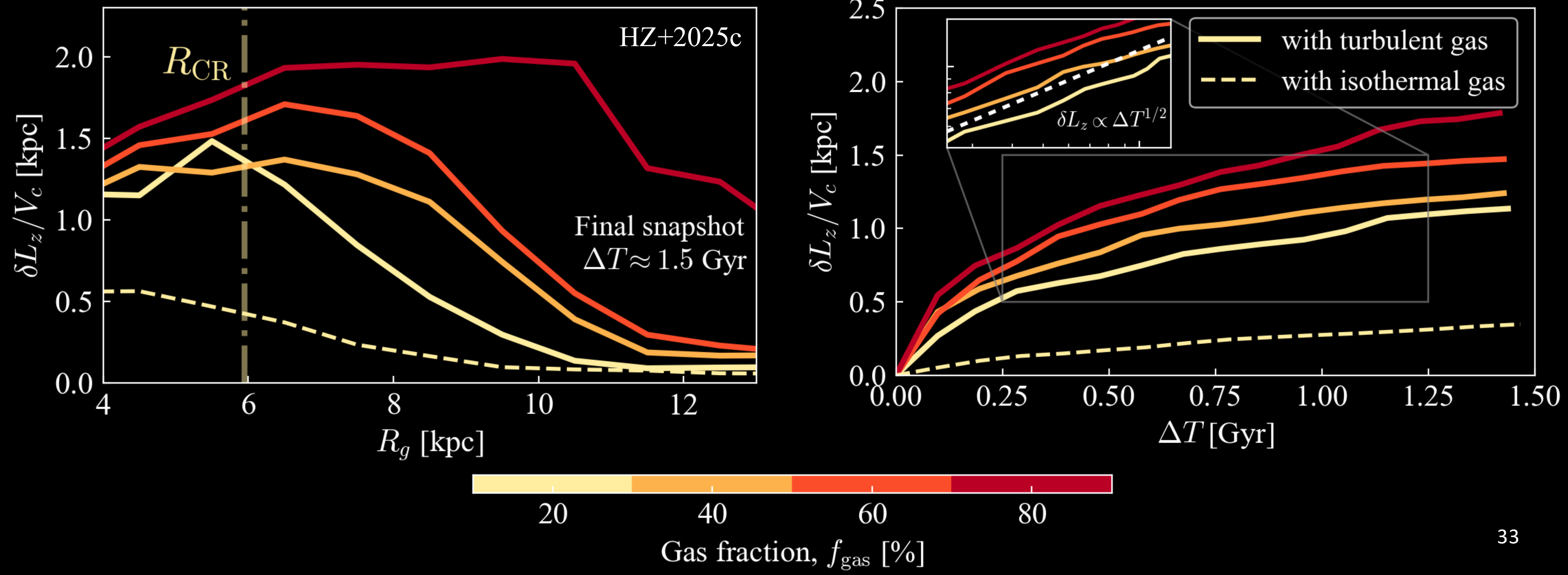

Possible interpretations of the transition in the radial migration strength from high$-\alpha$ to low$-\alpha$ disc

- Gas-rich to gas-poor disc transition when the low$-\alpha$ disc formed. (See also the evidence from kinematic fitting in Funakoshi+2025, and also supported by the high-z observation, Tsukui+2025)

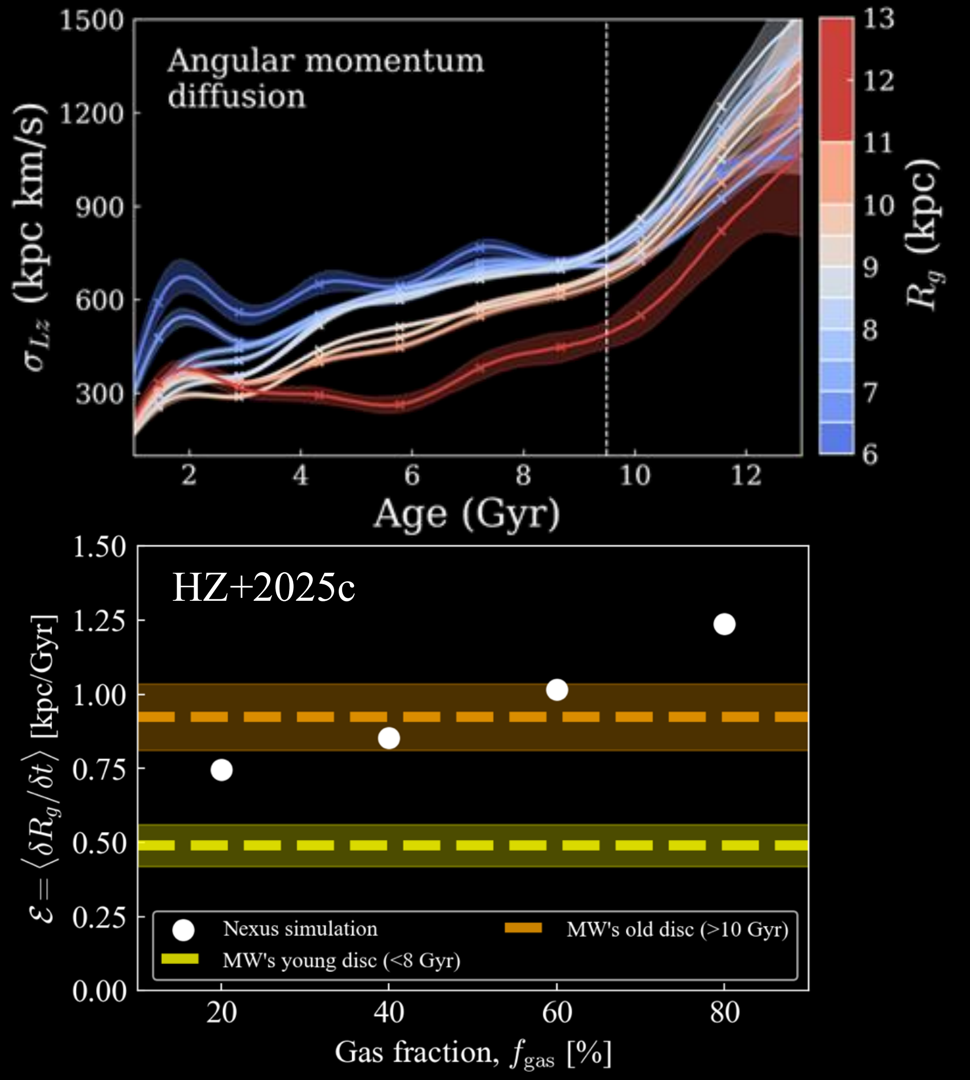

Possible interpretations of the transition in the radial migration strength from high$-\alpha$ to low$-\alpha$ disc

- Gas-rich to gas-poor disc transition when the low$-\alpha$ disc formed. (See also the evidence from kinematic fitting in Funakoshi+2025, and also supported by the high-z observation, Tsukui+2025)

- Bar-driven migration at the bar-formation epoch is also compatible with this result (Haywood+2024)

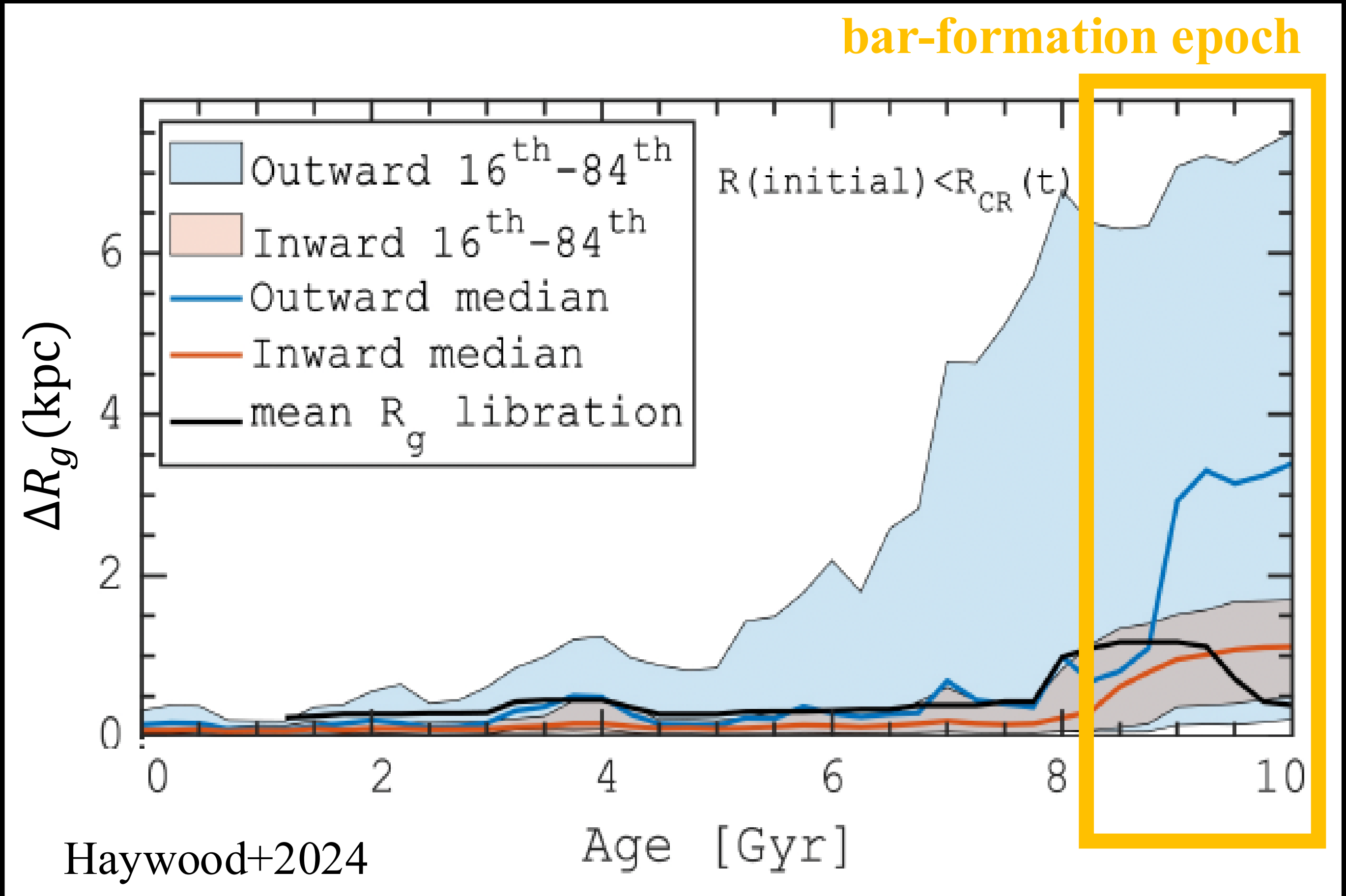

H. Zhang et al., 2025a, *ApJL* published
H. Zhang et al., 2025b&c, *MNRAS* submitted

Conclusion

- Importance of the decelerating bar to explain the chemo-chrono-dynamical pattern of the Milky Way, e.g. age-metallicity; α-bimodality; azimuthal metallicity features

- Modelling age-metallicity-kinematics space can uncover the birth properties of the disc, e.g. ISM metallicity gradient and star-forming disc scale length

- A transition of angular momentum diffusion coefficient appears around the high-α, and low-α disc transition, which could hint for a transition of the gas content in the Galaxy

- The low heating-to-migration ratio highlights the importance of corotation resonances in the secular evolution of the Galactic disc, and is consistent with the gas-poor disc in the Nexus simulations

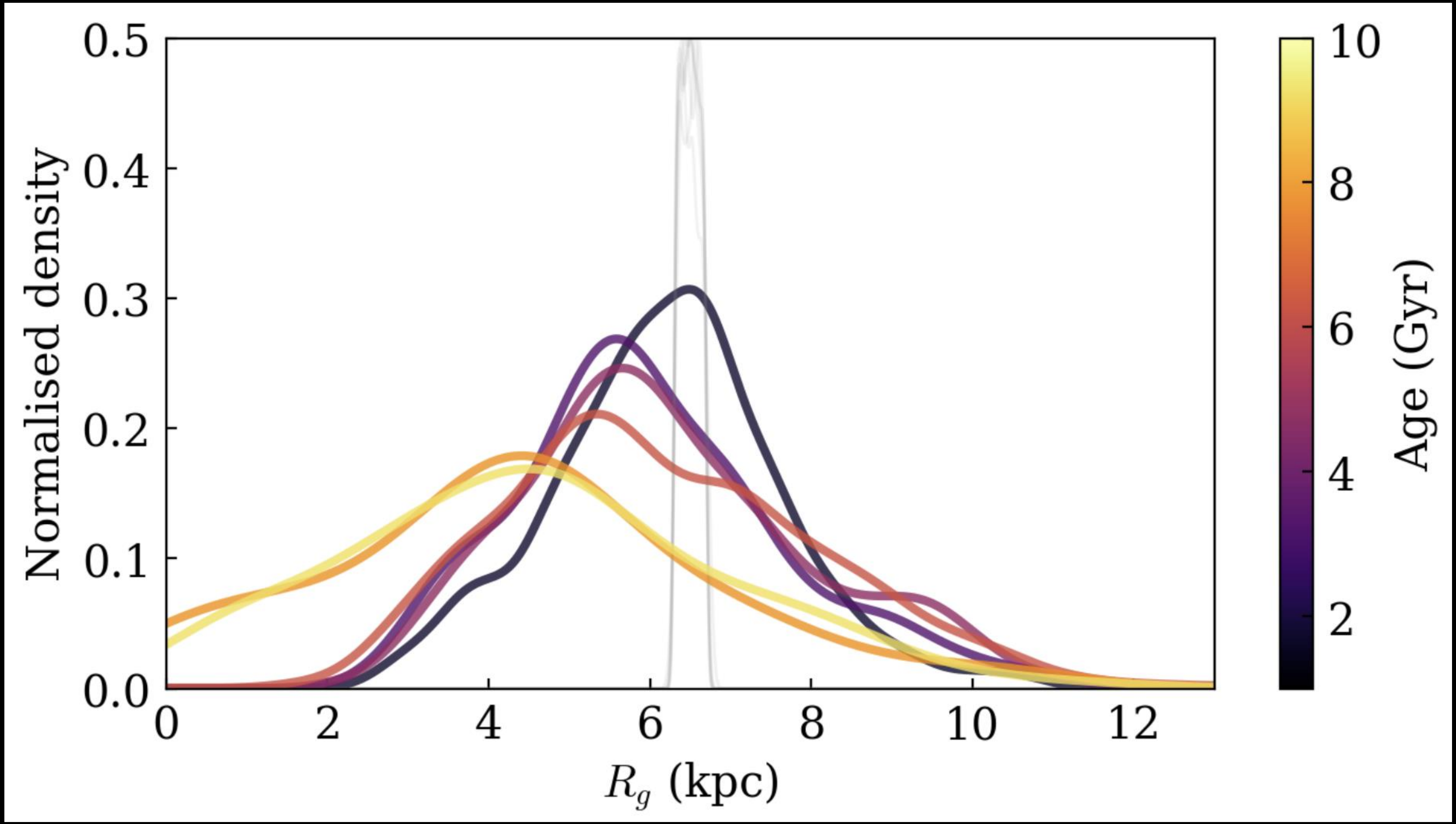

0.5
0.4
0.3
0.2
0.1
0.0
Normalised density
0
2
4
6
8
10
12
R_g (kpc)
10
8
6
4
2
Age (Gyr)

Density perturbation from gas

- Density perturbation averaged along the stellar orbits over the 1.5 Gyr

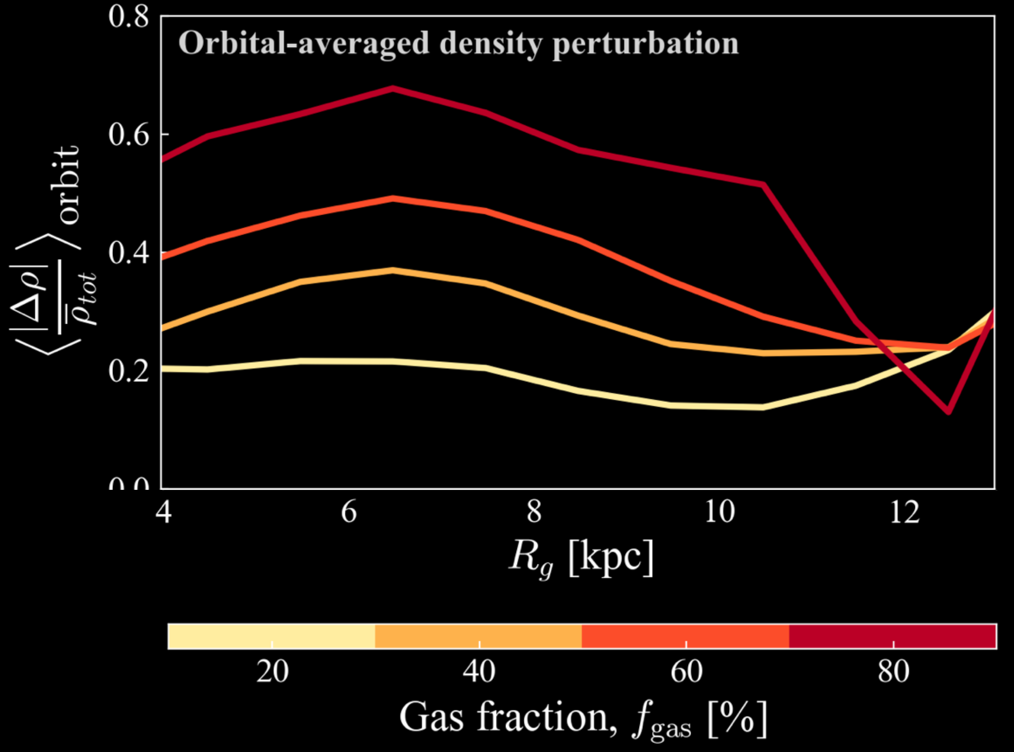

HZ+2025c

Density perturbation from gas

- Density perturbation averaged along the stellar orbits over the 1.5 Gyr
- Stars in the gas-rich disc encountered more perturbation from gas
- A transition between 20-40% where the perturbation of gas becomes more significant than the stars

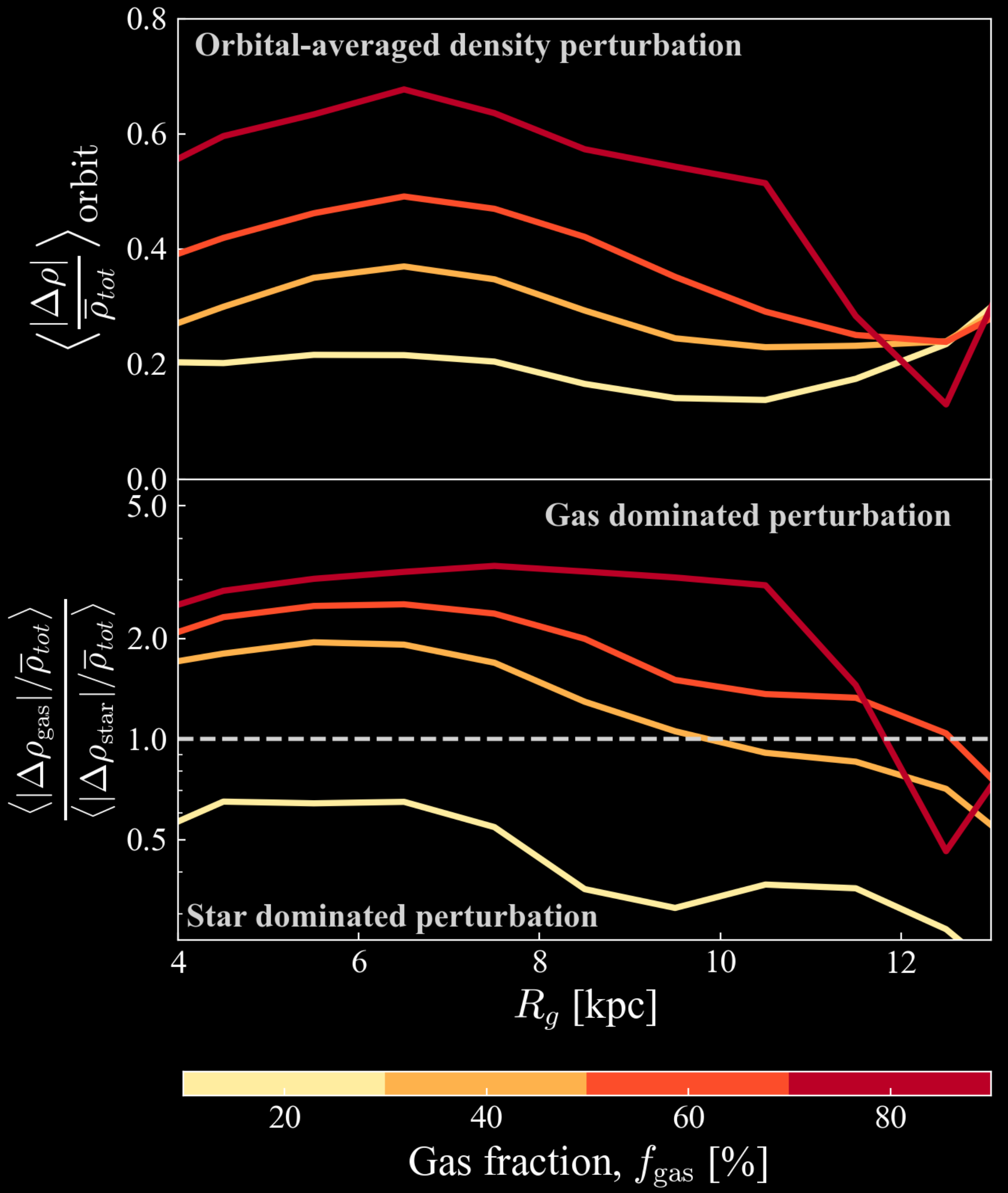

HZ+2025c

Spectrograms of m=2 mode

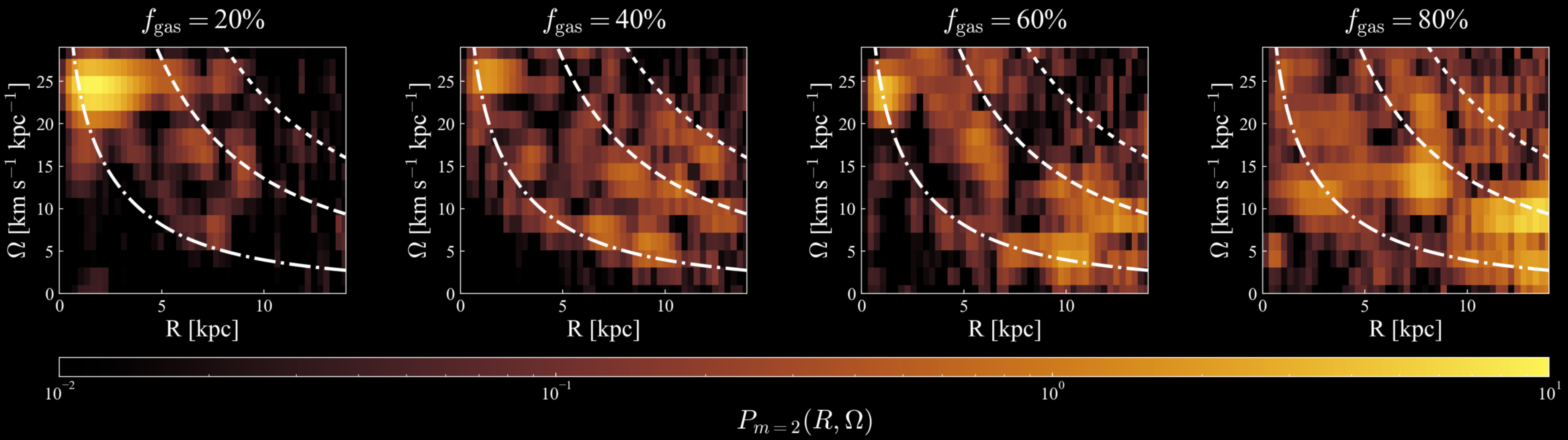

HZ+2025c

Impact from gas on different migration mechanisms

In a more gas-rich galaxy

1. Less radial transportation from corotation resonance dragging
2. More outward migration to the OLR barrier
3. Also, more migration for stars outside OLR

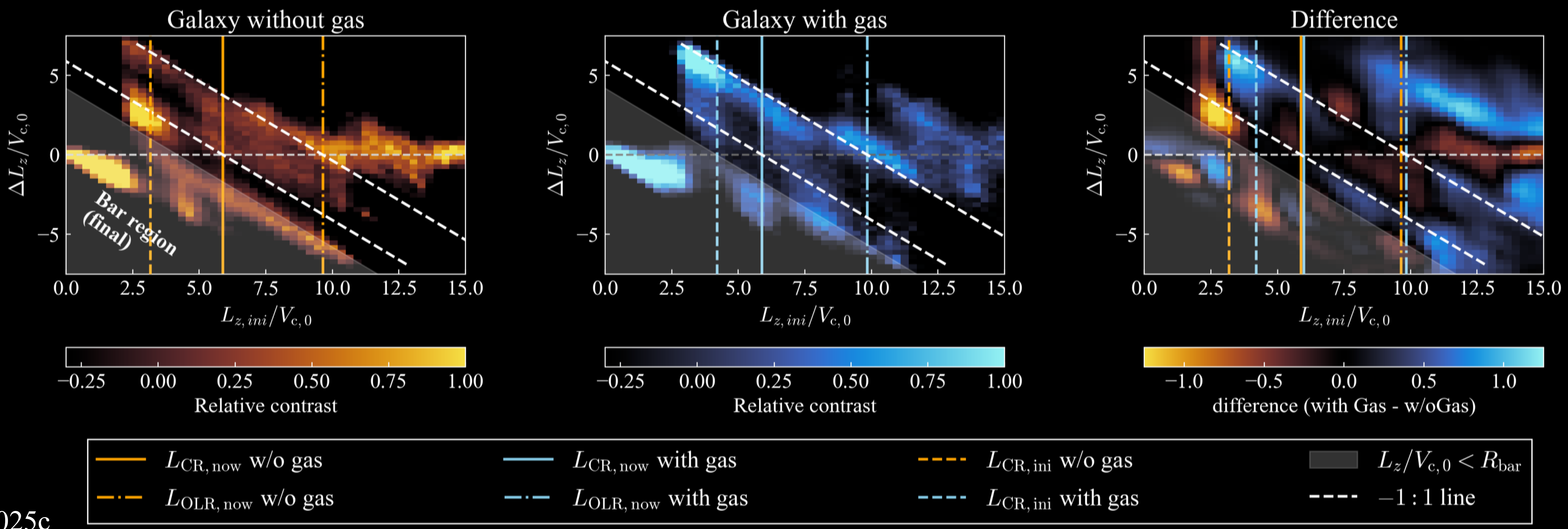

HZ+2025c

Future direction

- Secular evolution of the inner region of the Milky Way: applying the model to the reconstructed Milky Way with the orbital superposition method (Khoperskov+2025)

- Adding vertical metallicity gradient to the model, inspired by Kawata+(2018)

- Quantify the relation between the spectrogram of the galaxy with the secular evolution history and observable quantities

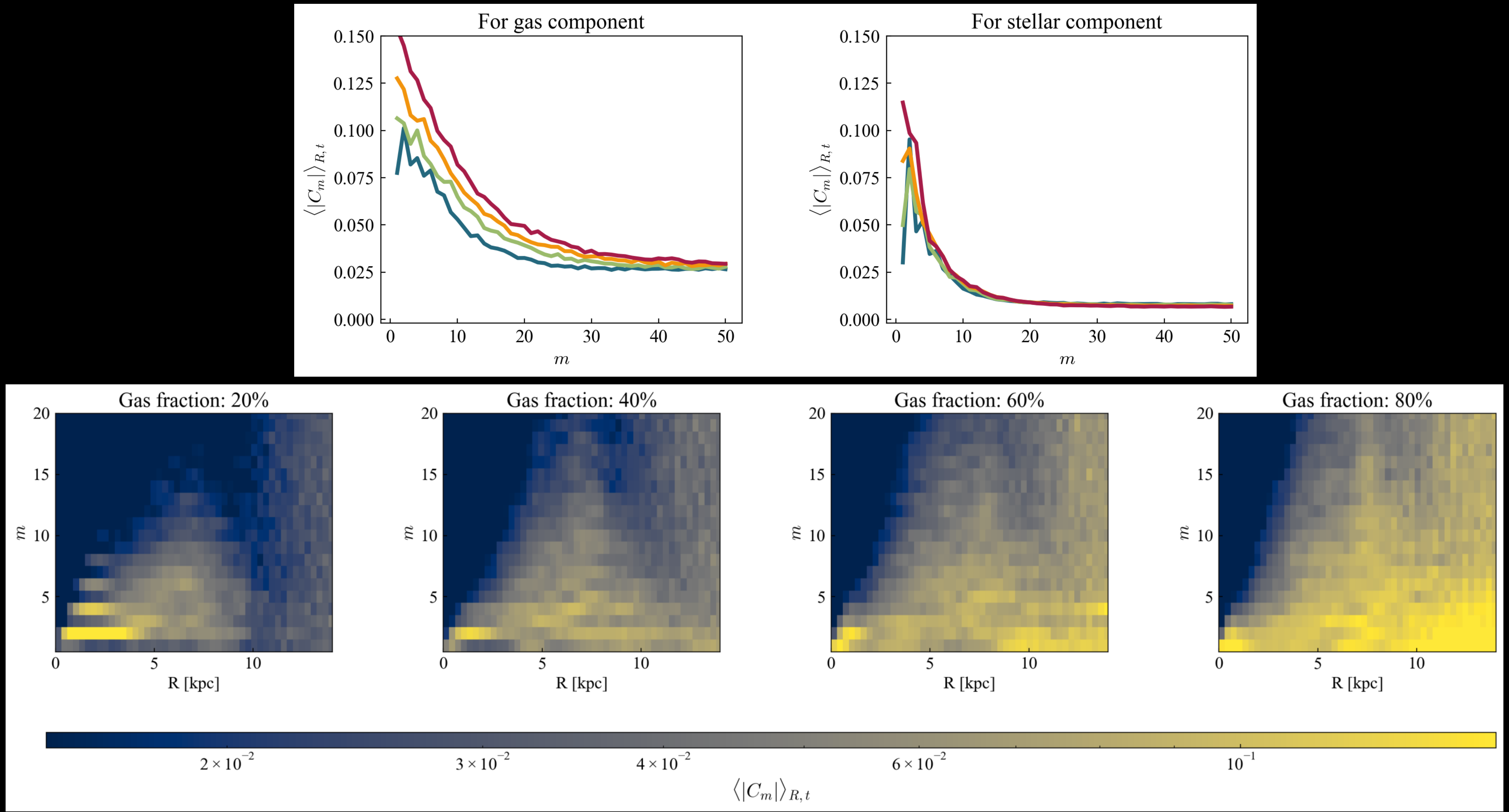
For gas component
For stellar component
$\langle|C_m|\rangle_{R,t}$
m
0.000
0.025
0.050
0.075
0.100
0.125
0.150
0
10
20
30
40
50
Gas fraction: 20%
Gas fraction: 40%
Gas fraction: 60%
Gas fraction: 80%
R [kpc]
2×10^{-2}
3×10^{-2}
4×10^{-2}
6×10^{-2}
10^{-1}

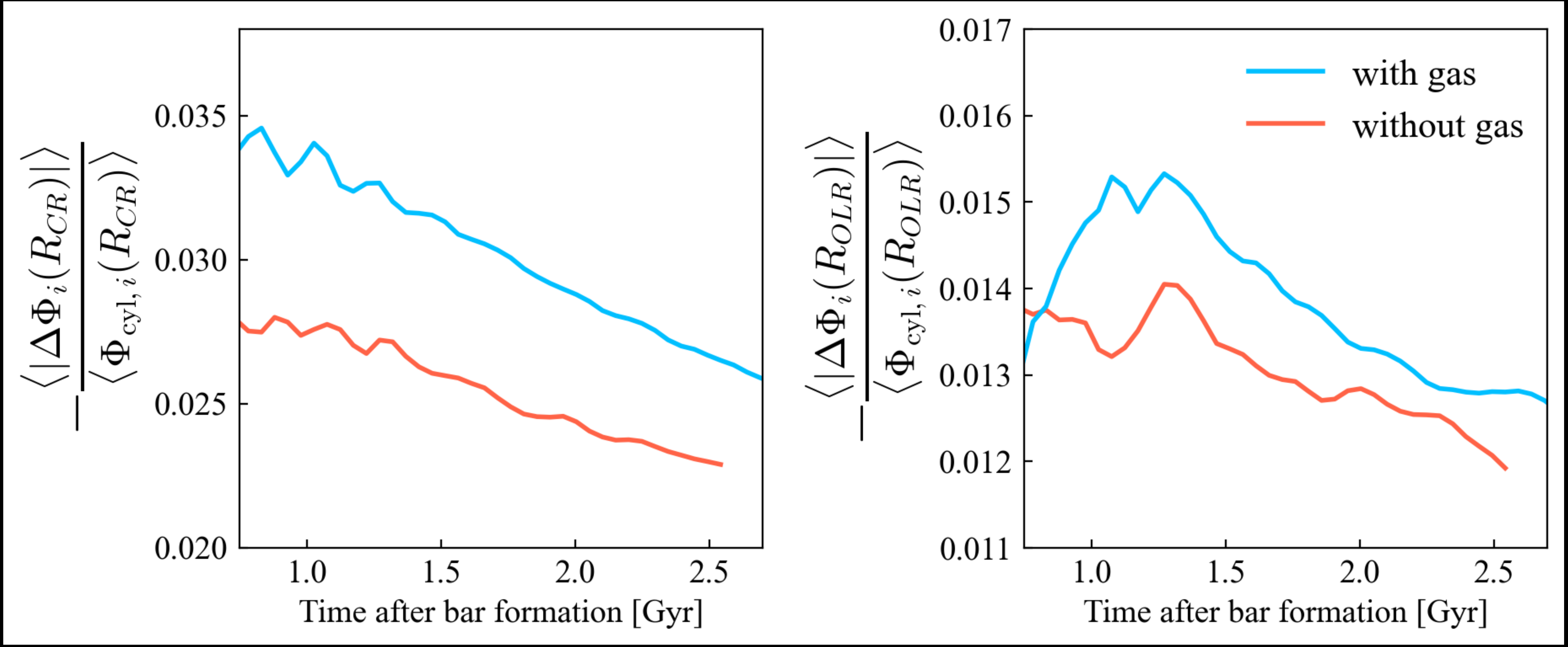

0.035
0.030
0.025
0.020
1.0
1.5
2.0
2.5
Time after bar formation [Gyr]
0.017
0.016
0.015
0.014
0.013
0.012
0.011
1.0
1.5
2.0
2.5
Time after bar formation [Gyr]
with gas
without gas

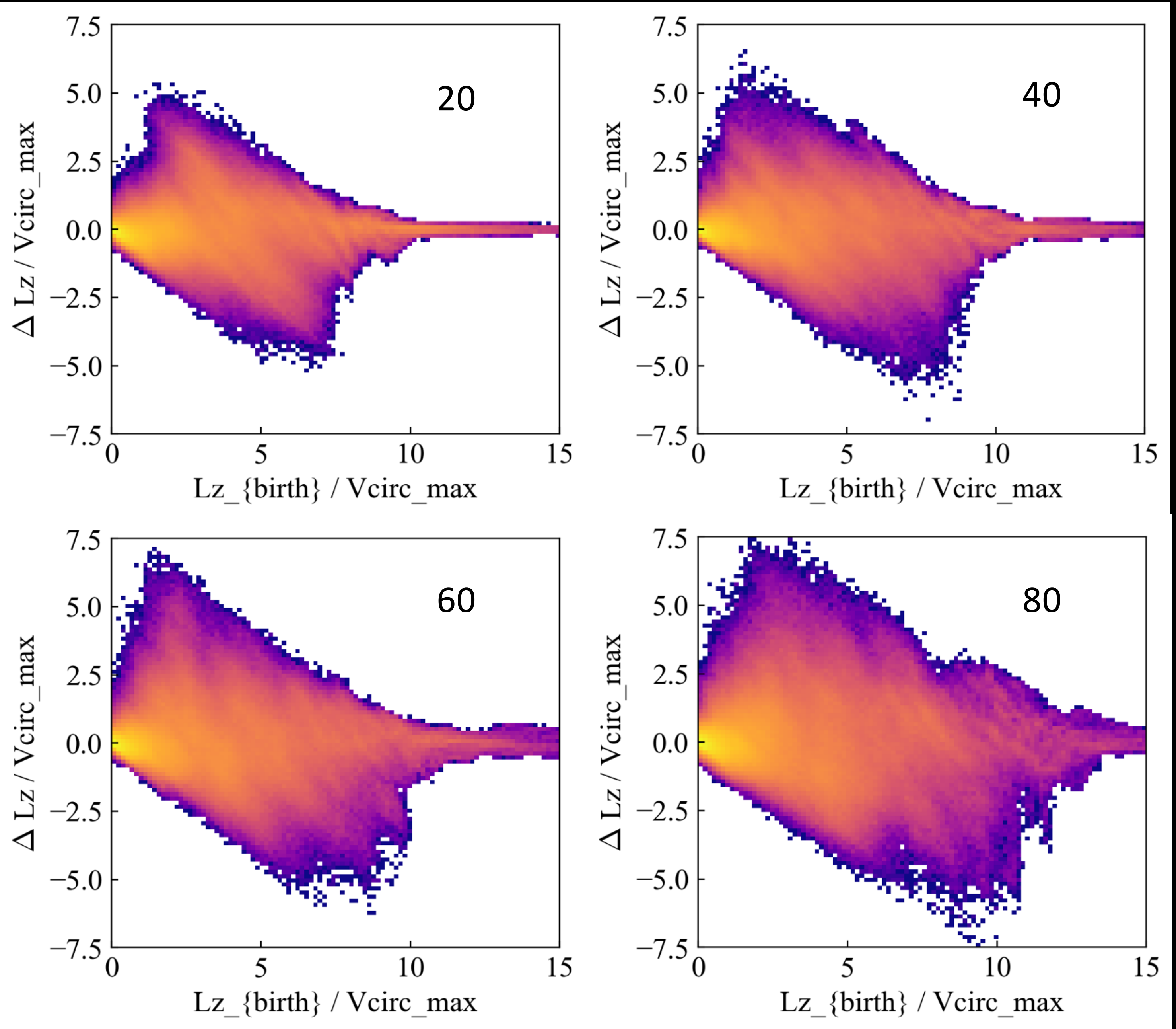
20
40
60
80
Δ Lz / Vcirc_max
Lz_{birth} / Vcirc_max

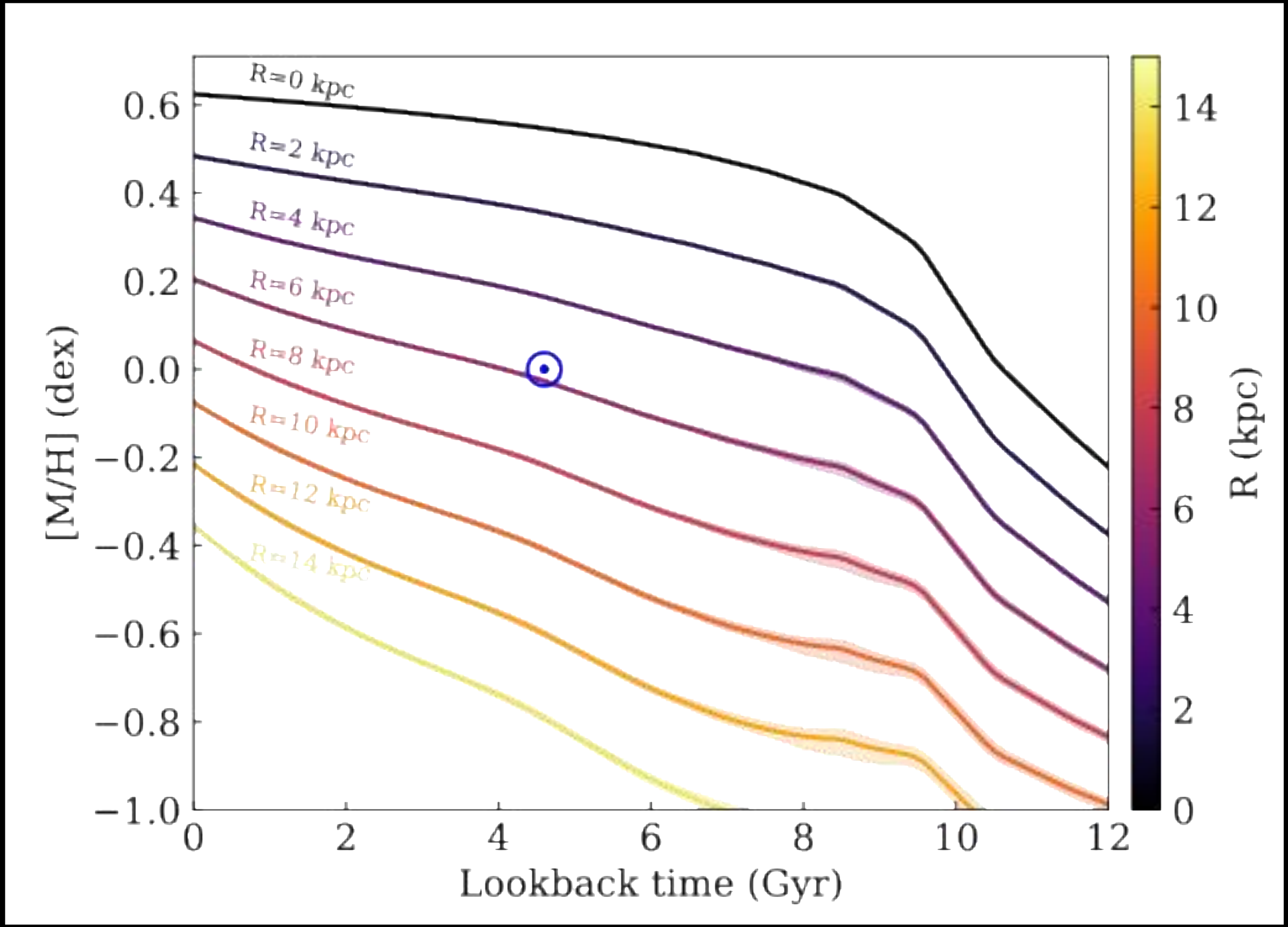

R=0 kpc
R=2 kpc
R=4 kpc
R=6 kpc
R=8 kpc
R=10 kpc
R=12 kpc
R=14 kpc
0.6
0.4
0.2
0.0
−0.2
−0.4
−0.6
−0.8
−1.0
[M/H] (dex)
0
2
4
6
8
10
12
Lookback time (Gyr)
14
12
10
8
6
4
2
0
R (kpc)

Sanity check: azimuthal metallicity dispersion

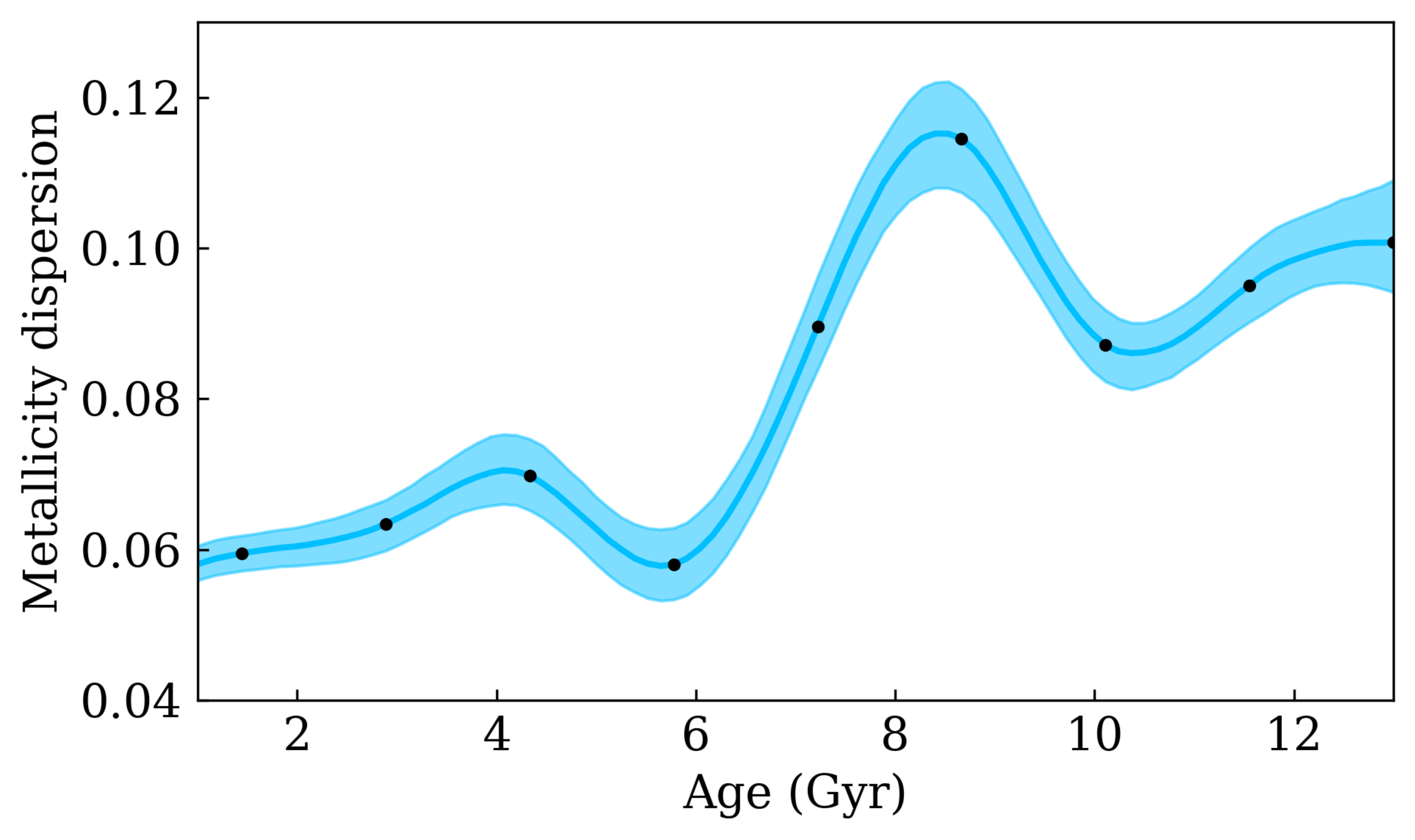

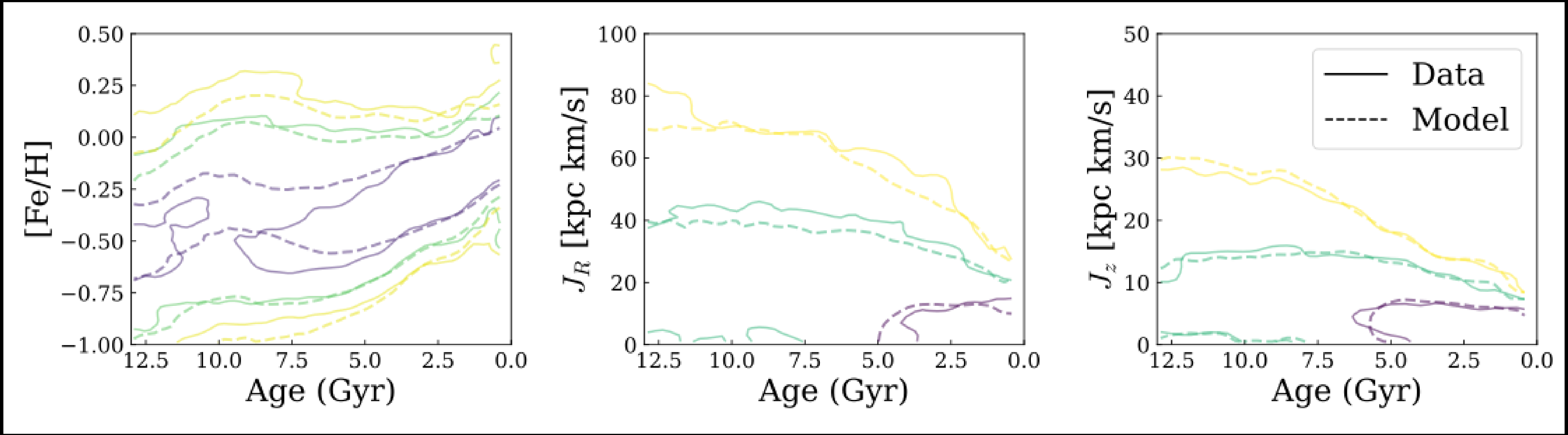

0.50
0.25
0.00
−0.25
−0.50
−0.75
−1.00
[Fe/H]
12.5
10.0
7.5
5.0
2.5
0.0
Age (Gyr)
100
80
60
40
20
0
J_R [kpc km/s]
Age (Gyr)
50
40
30
20
10
0
J_z [kpc km/s]
Age (Gyr)
Data
Model

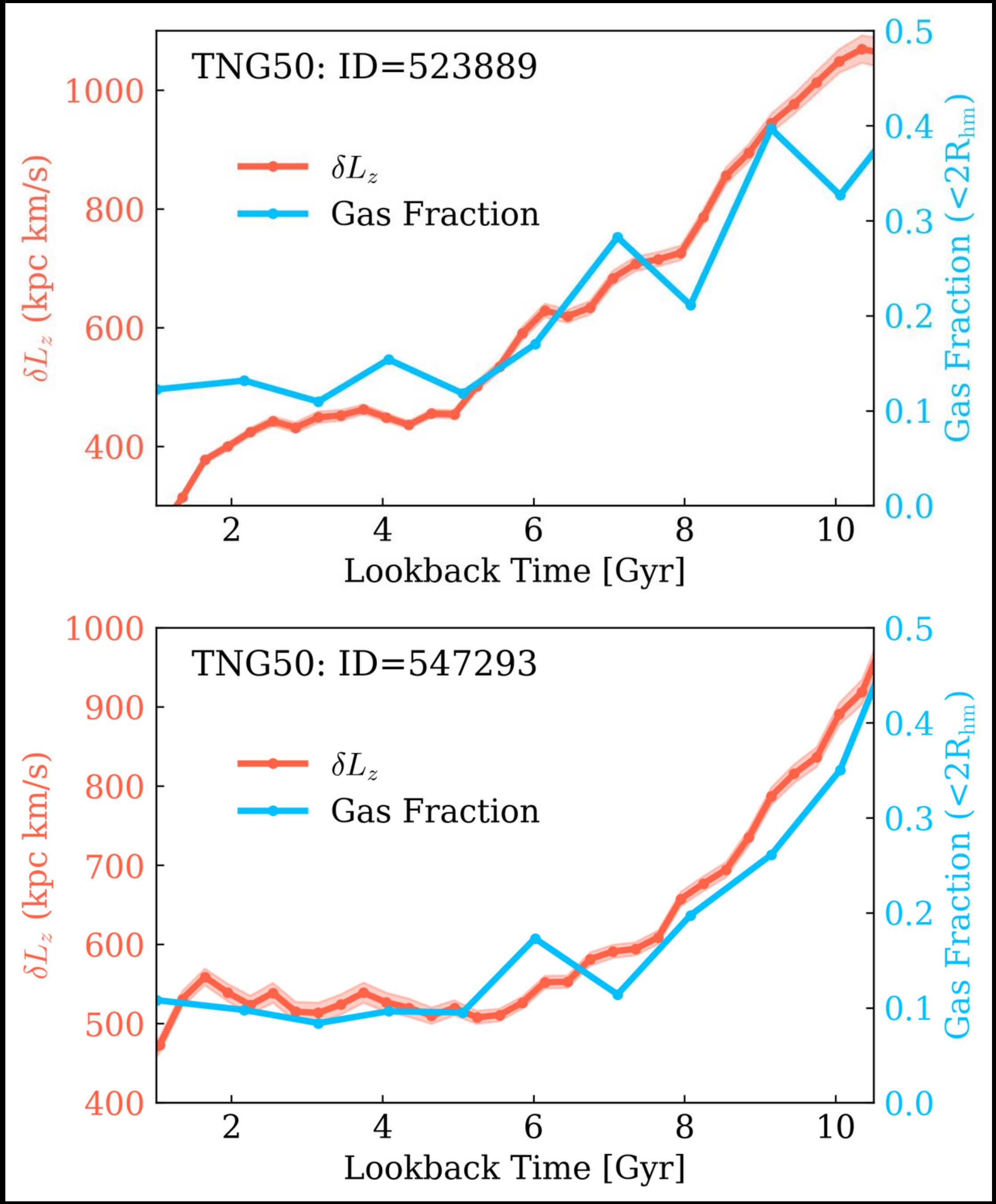

TNG50: ID=523889
δL_z
Gas Fraction
δL_z (kpc km/s)
Gas Fraction (<2R$_{\rm hm}$)
1000
800
600
400
0.5
0.4
0.3
0.2
0.1
0.0
2
4
6
8
10
Lookback Time [Gyr]
TNG50: ID=547293
δL_z
Gas Fraction
δL_z (kpc km/s)
Gas Fraction (<2R$_{\rm hm}$)
1000
900
800
700
600
500
400
0.5
0.4
0.3
0.2
0.1
0.0
2
4
6
8
10
Lookback Time [Gyr]

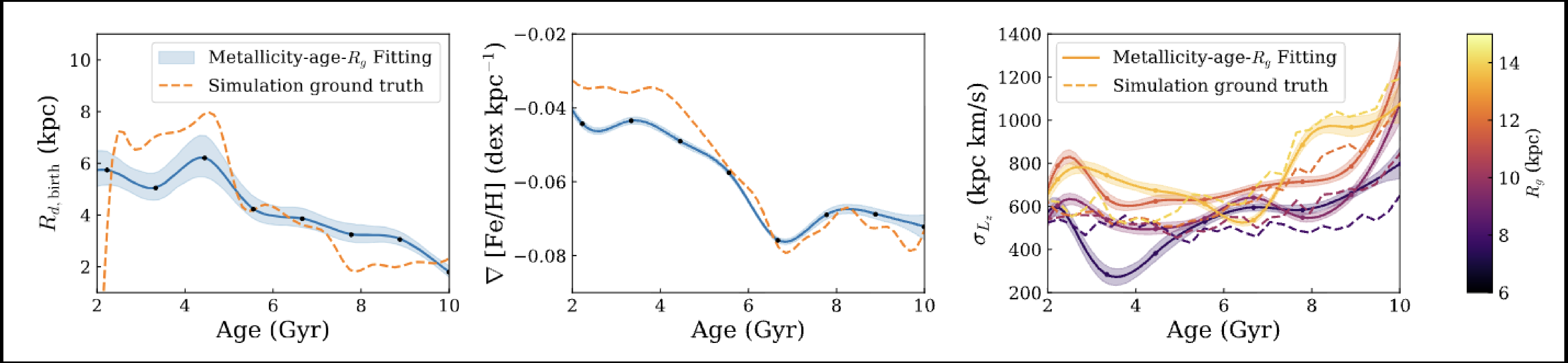
Metallicity-age-R_g Fitting
Simulation ground truth
$R_{d,\,\mathrm{birth}}$ (kpc)
Age (Gyr)
∇ [Fe/H] (dex kpc^{-1})
Age (Gyr)
Metallicity-age-R_g Fitting
Simulation ground truth
σ_{L_z} (kpc km/s)
Age (Gyr)
R_g (kpc)

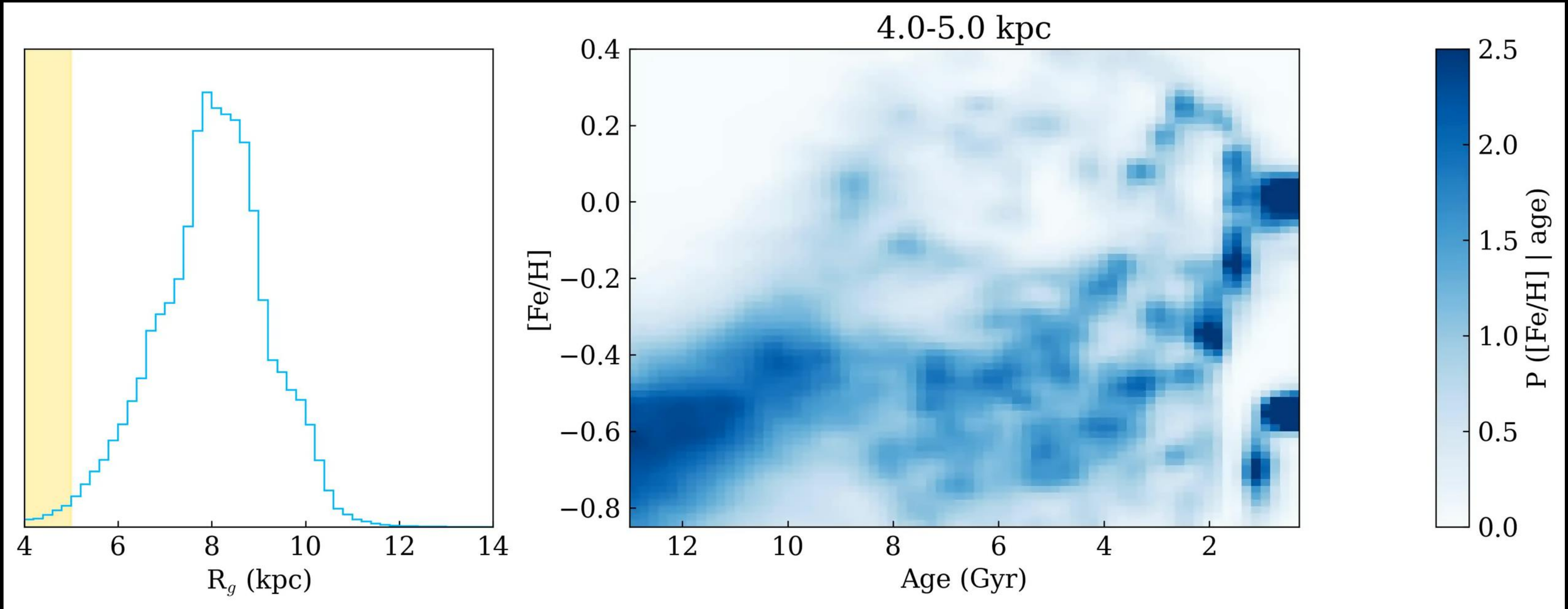

4.0-5.0 kpc
R_g (kpc)
Age (Gyr)
[Fe/H]
P ([Fe/H] | age)
4
6
8
10
12
14
0.4
0.2
0.0
−0.2
−0.4
−0.6
−0.8
12
10
8
6
4
2
2.5
2.0
1.5
1.0
0.5
0.0

Resulting age-metallicity sequences

The guiding radii dependence

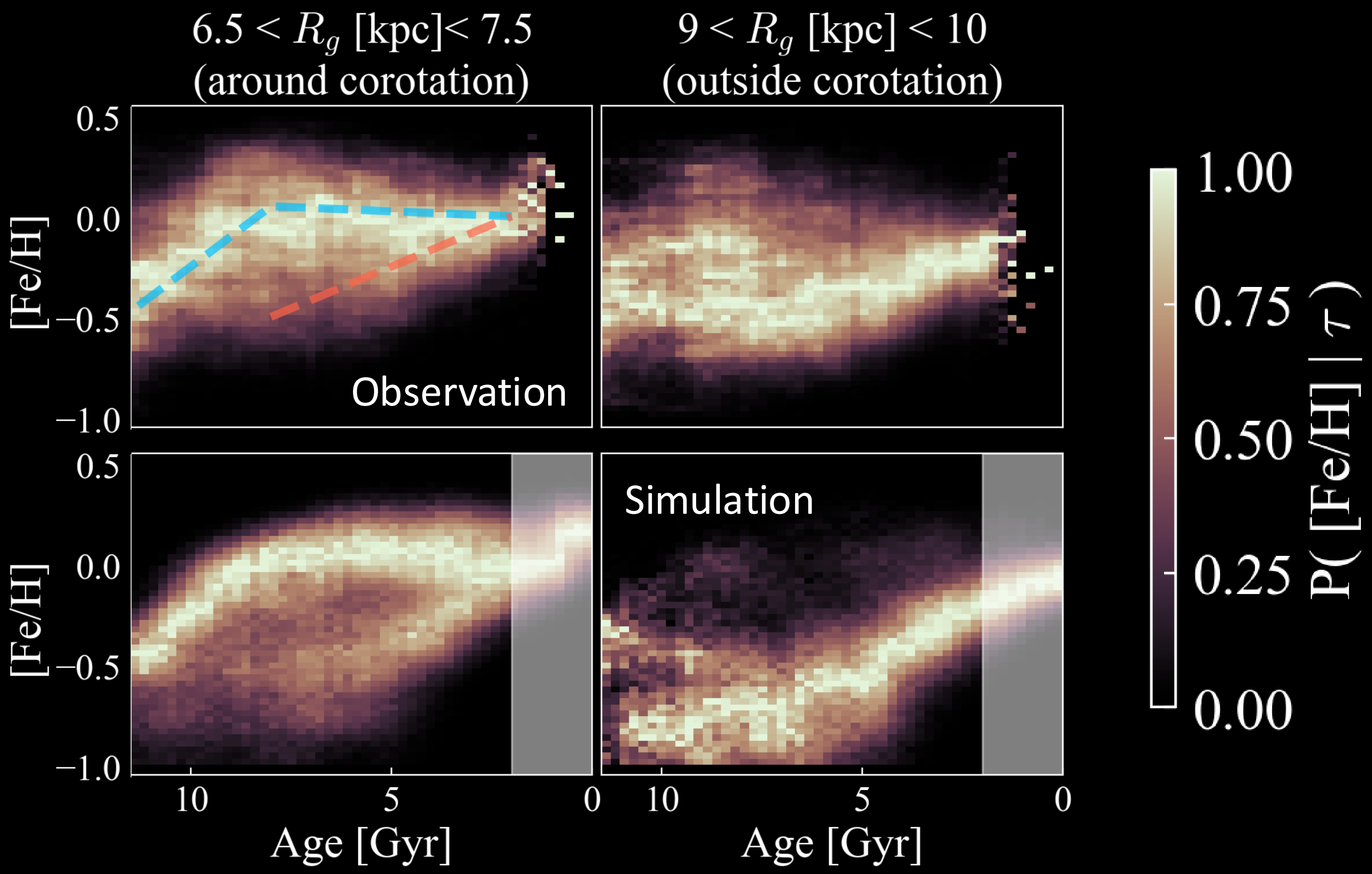

HZ+2025

Resonant dragging of a decelerating bar

A quick introduction

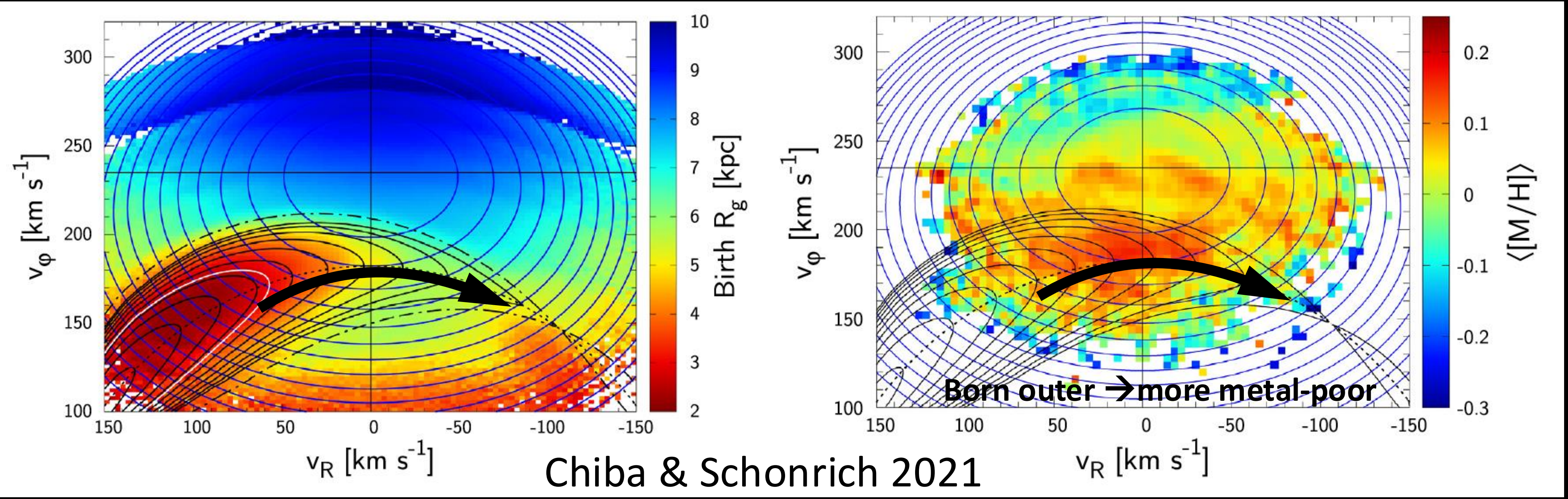

Chiba & Schonrich 2021

Today's bar pattern speed: $\Omega_b \sim 33 - 37$ km/s/kpc (Chiba+21; Clarke+22; Zhang+24 ; Dillamore+24, 25) → Corotation radius $R_{CR} \sim 6.2 - 7.0$ kpc

Resonant dragging of a decelerating bar

Test-particle simulation setup

This is adopted from Lu+24, which calibrated with observed Milky Way's metallicity pattern

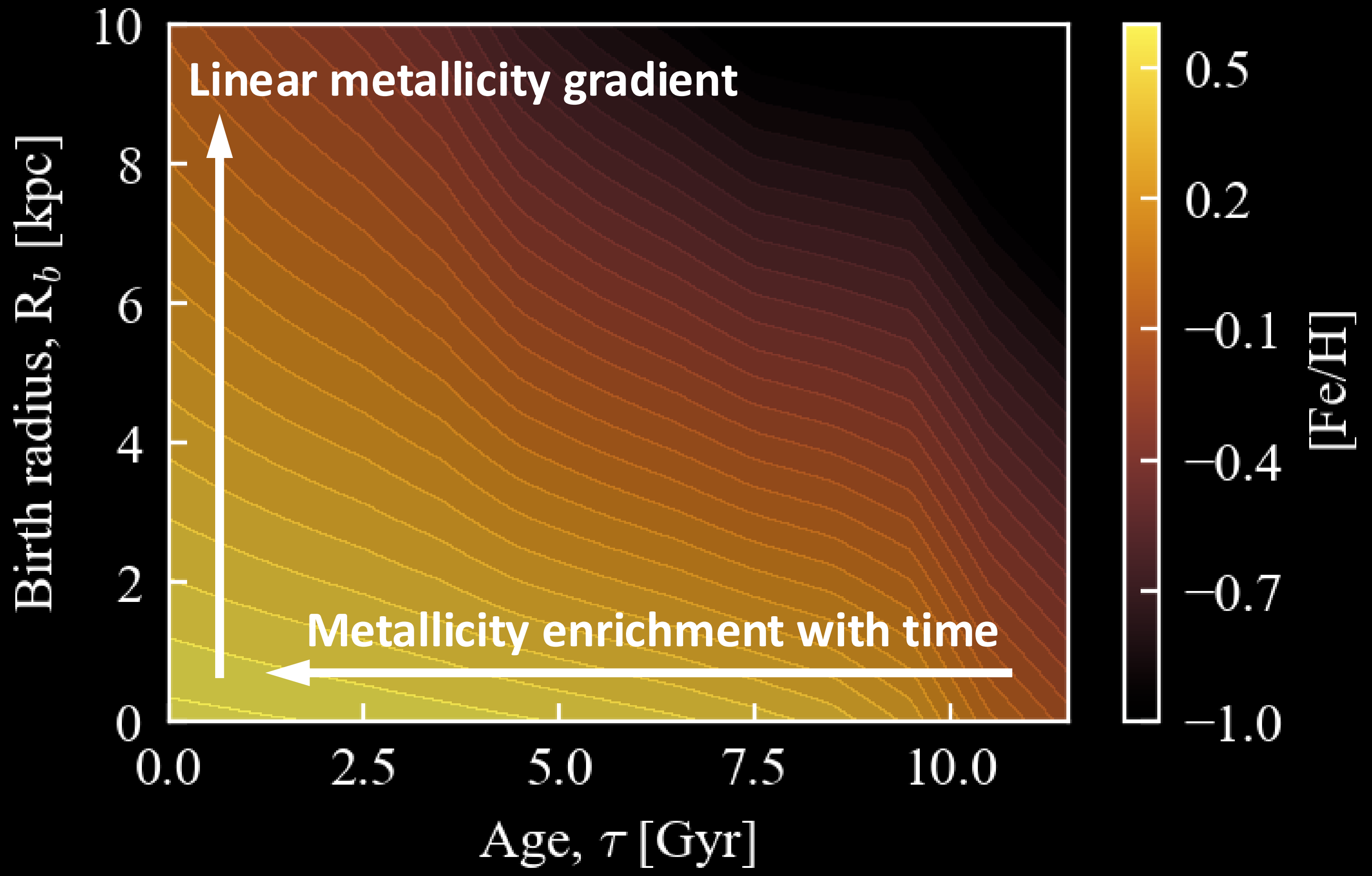

Implications: 3) Broken power-law in stellar density

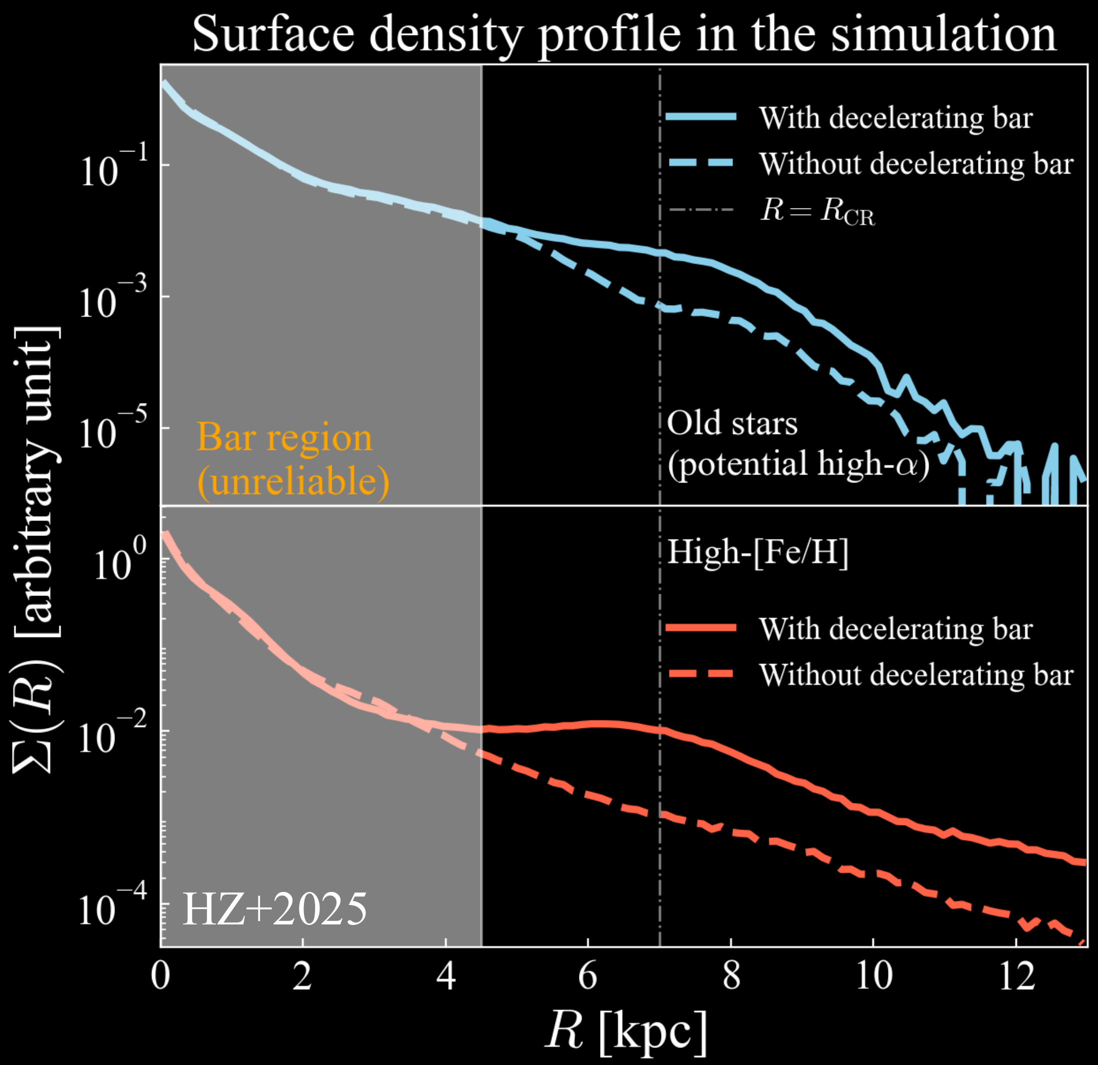

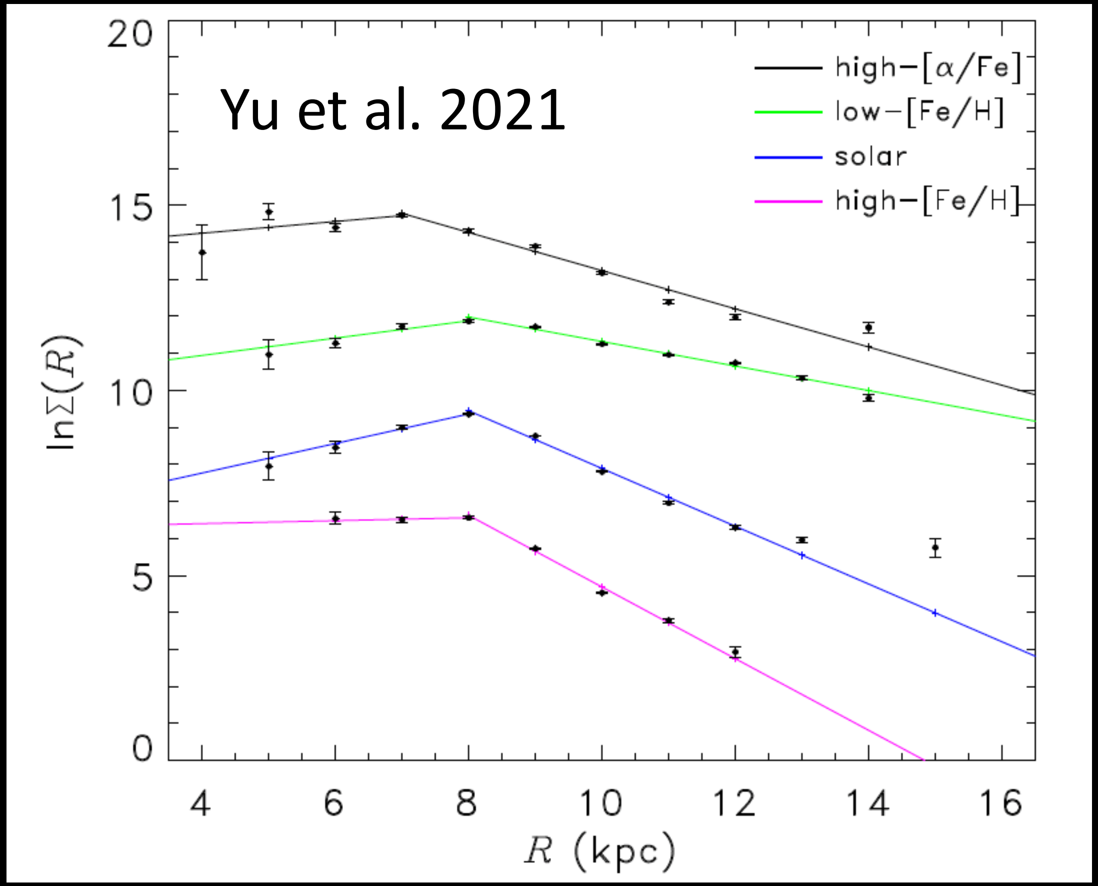

See also Bovy+15, Lian+22

Implications: 4) Coldness of the disc

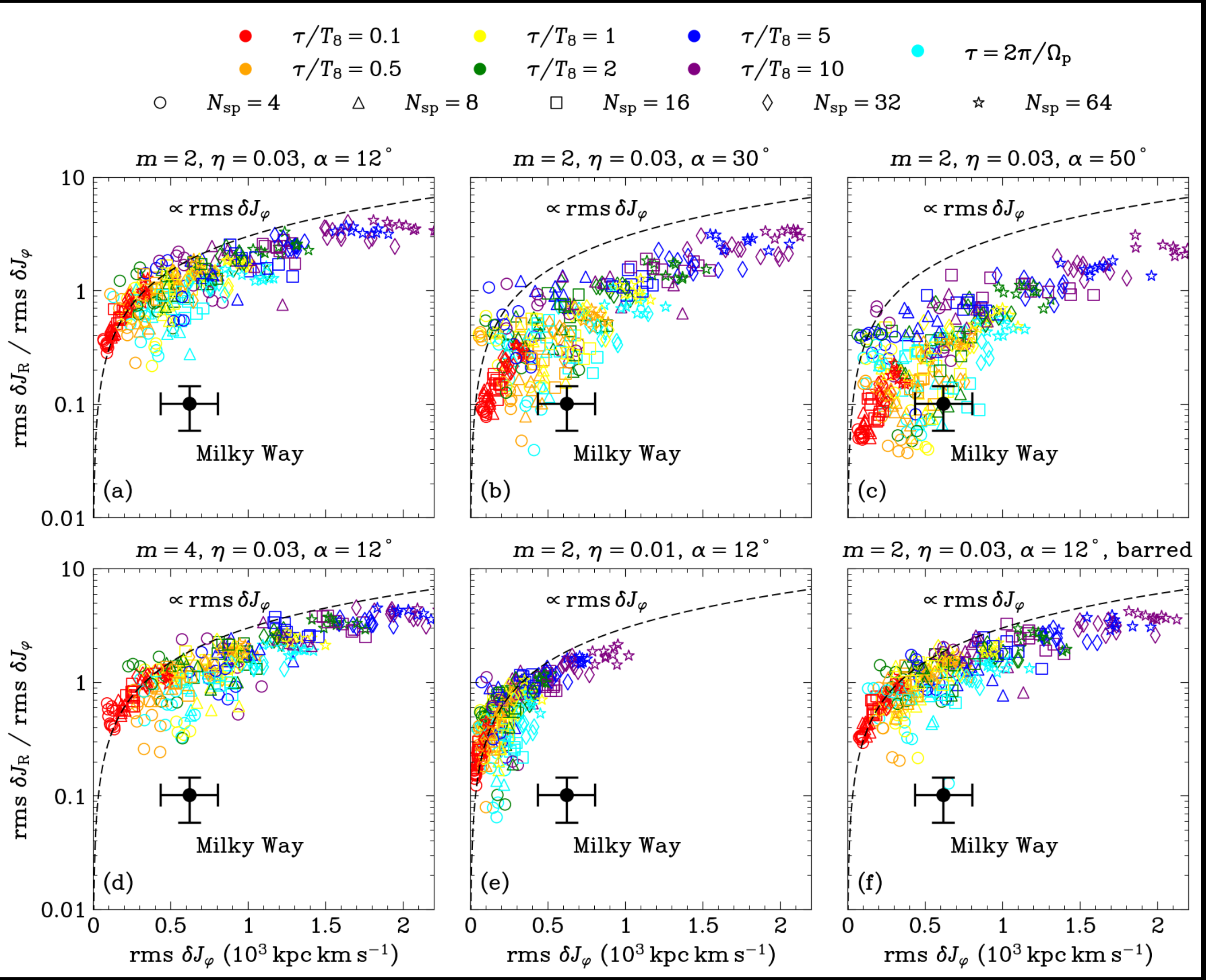

Hamilton et al. 2024

The Milky Way observation is from Frankel+20

But see also the demonstration in Sellwood & Binney 2025

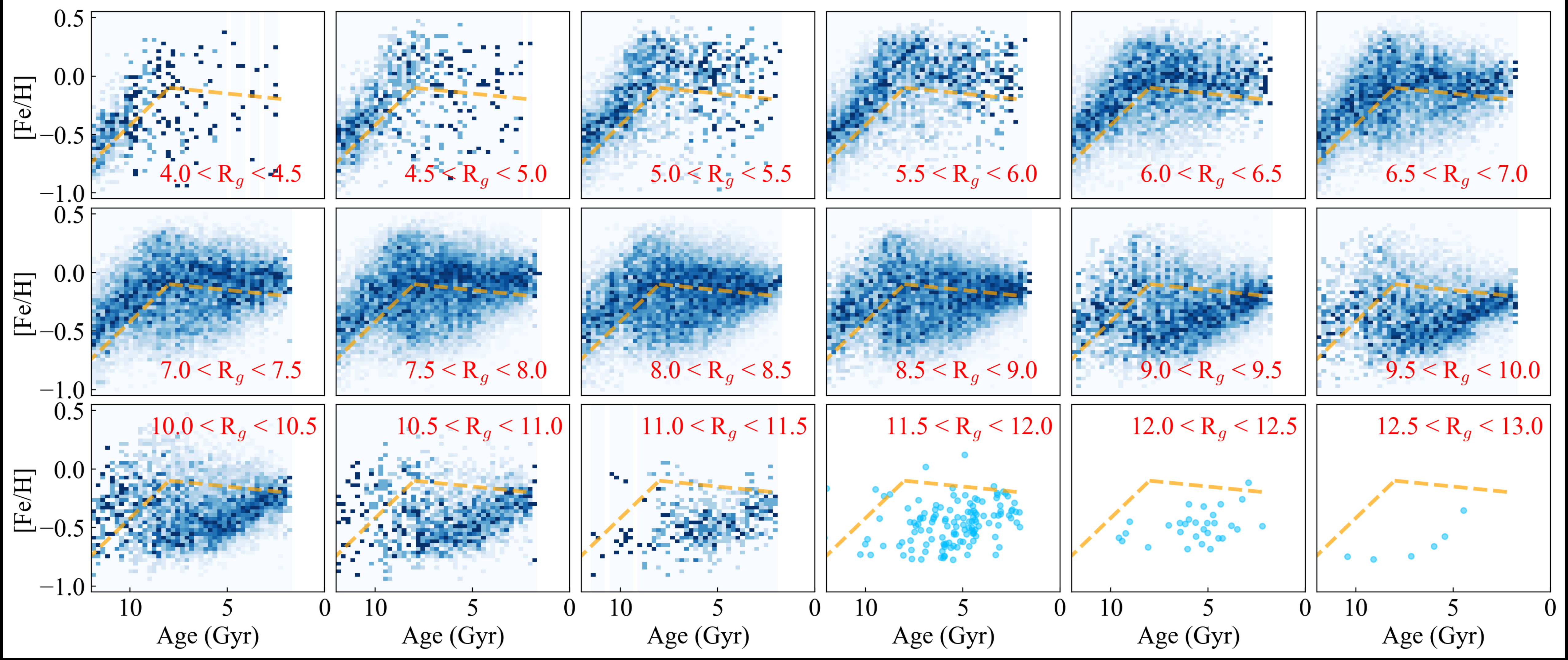

[Fe/H]
Age (Gyr)
4.0 < R_g < 4.5
4.5 < R_g < 5.0
5.0 < R_g < 5.5
5.5 < R_g < 6.0
6.0 < R_g < 6.5
6.5 < R_g < 7.0
7.0 < R_g < 7.5
7.5 < R_g < 8.0
8.0 < R_g < 8.5
8.5 < R_g < 9.0
9.0 < R_g < 9.5
9.5 < R_g < 10.0
10.0 < R_g < 10.5
10.5 < R_g < 11.0
11.0 < R_g < 11.5
11.5 < R_g < 12.0
12.0 < R_g < 12.5
12.5 < R_g < 13.0

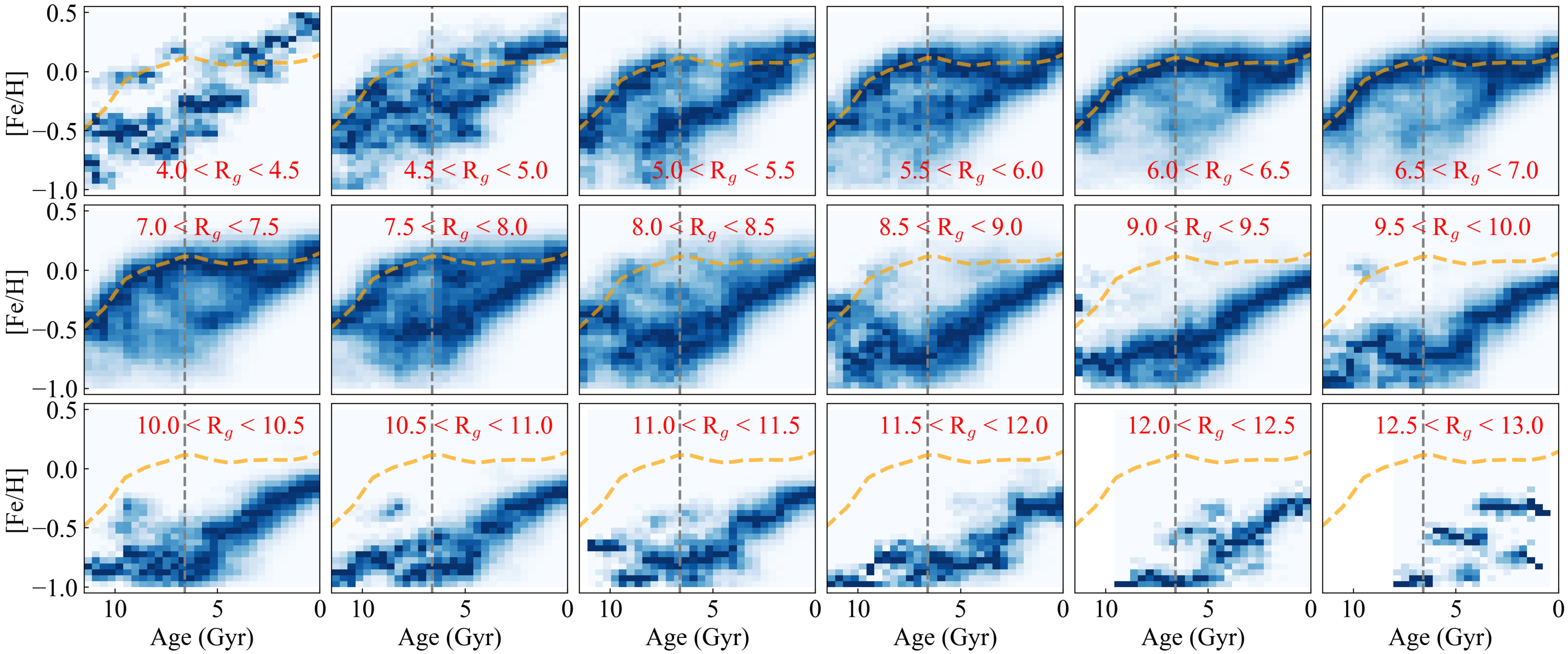

[Fe/H]
Age (Gyr)
4.0 < R_g < 4.5
4.5 < R_g < 5.0
5.0 < R_g < 5.5
5.5 < R_g < 6.0
6.0 < R_g < 6.5
6.5 < R_g < 7.0
7.0 < R_g < 7.5
7.5 < R_g < 8.0
8.0 < R_g < 8.5
8.5 < R_g < 9.0
9.0 < R_g < 9.5
9.5 < R_g < 10.0
10.0 < R_g < 10.5
10.5 < R_g < 11.0
11.0 < R_g < 11.5
11.5 < R_g < 12.0
12.0 < R_g < 12.5
12.5 < R_g < 13.0

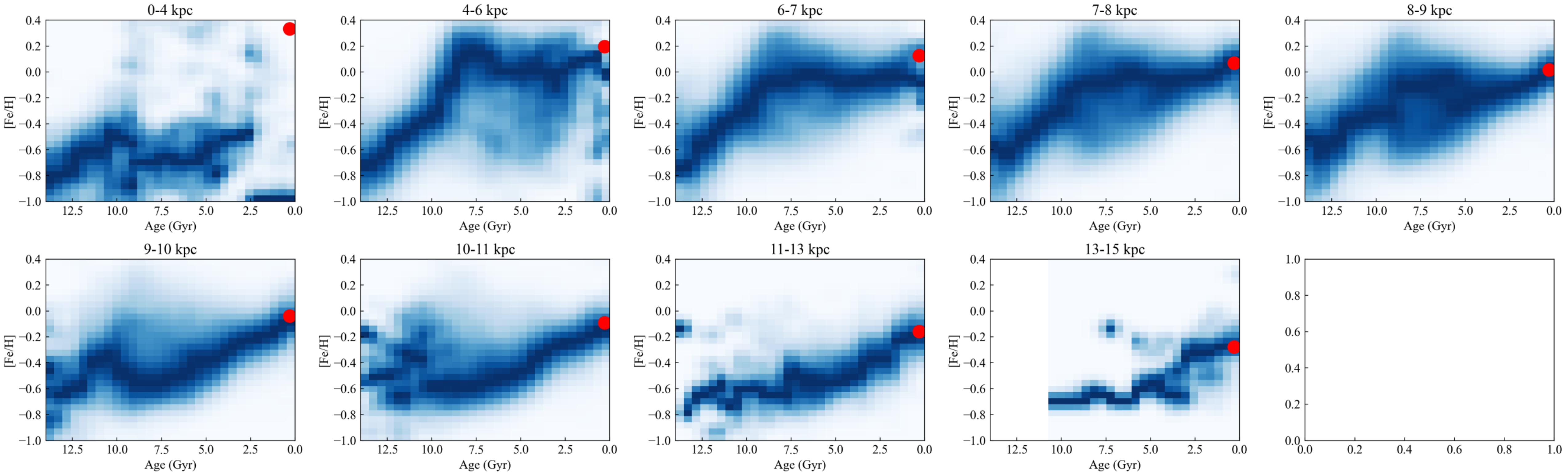

0-4 kpc
4-6 kpc
6-7 kpc
7-8 kpc
8-9 kpc
9-10 kpc
10-11 kpc
11-13 kpc
13-15 kpc
[Fe/H]
Age (Gyr)

Implications: 2) Azimuthal patterns

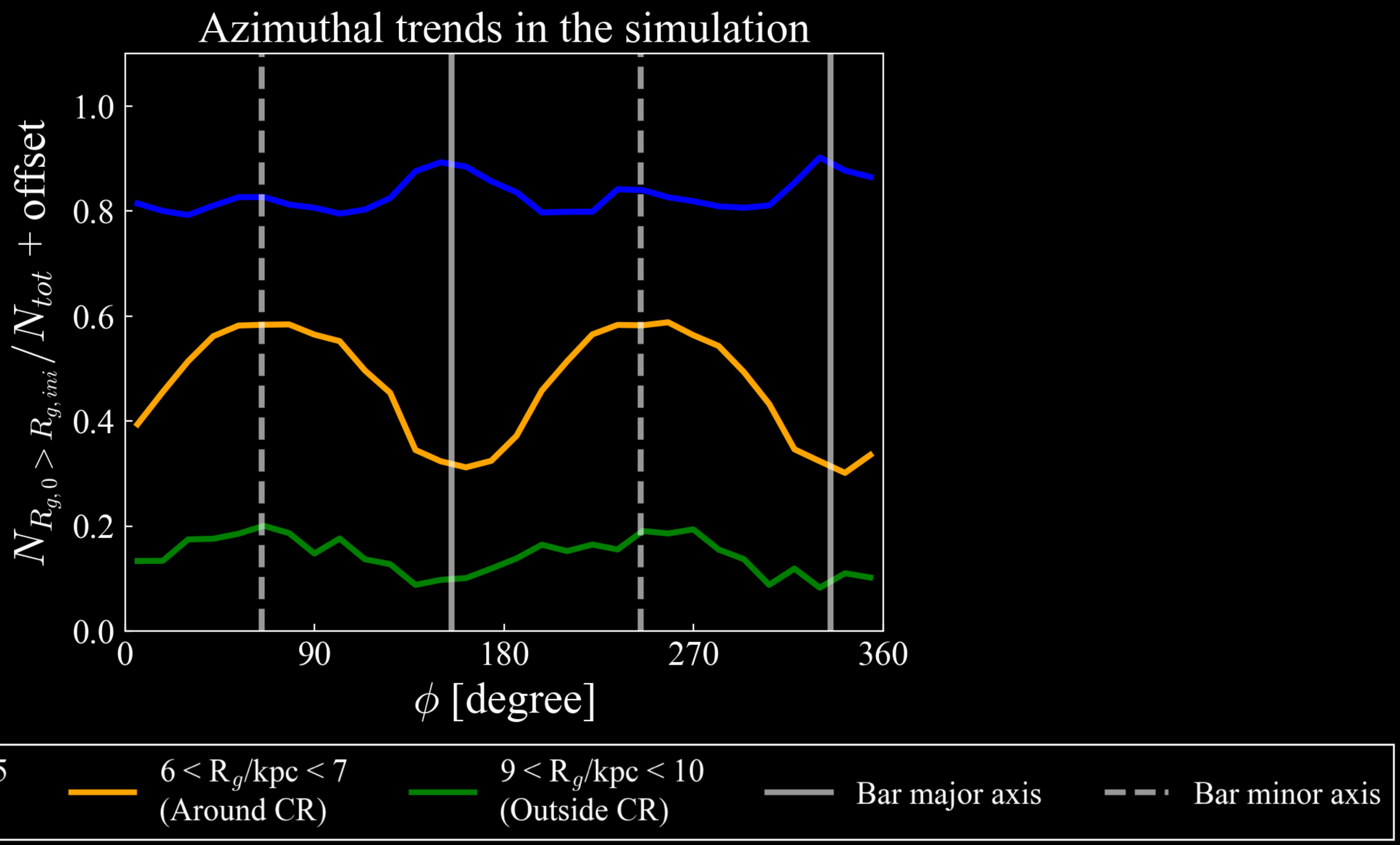

HZ+2025

Implications: 2) Azimuthal patterns

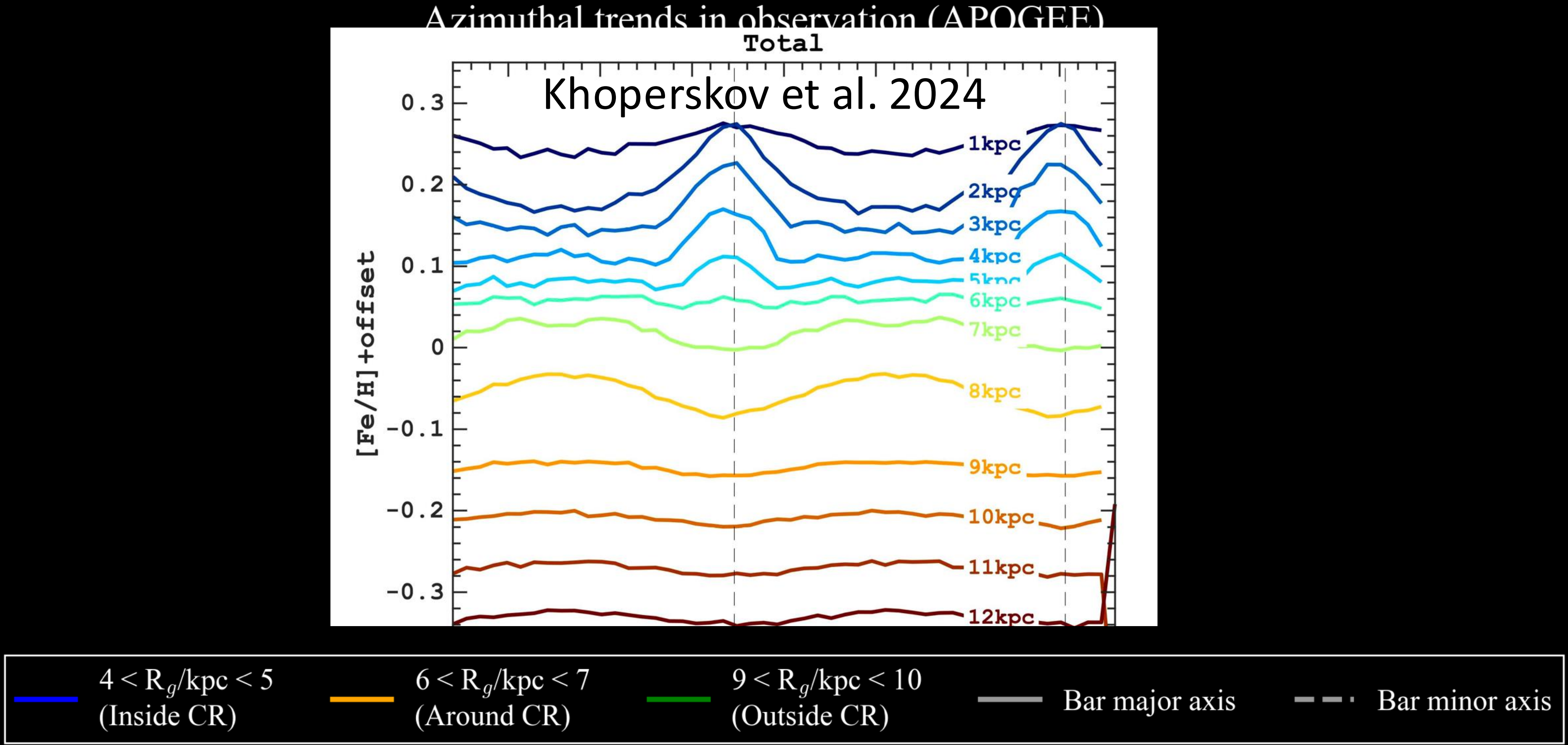

HZ+2025

See also Poggio+23, Hawkins 2023, Hackshaw+24

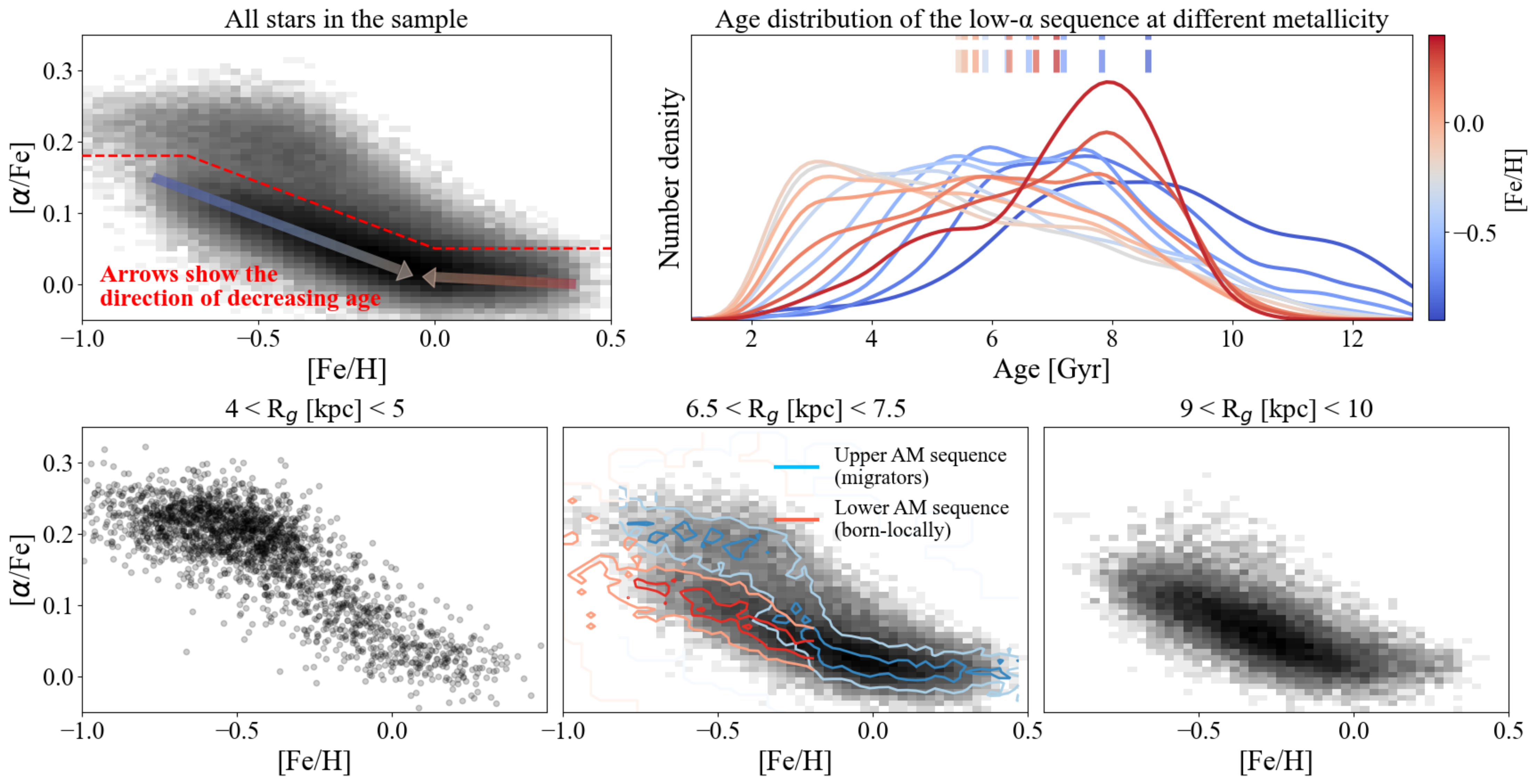

All stars in the sample
[α/Fe]
[Fe/H]
Arrows show the direction of decreasing age
Age distribution of the low-α sequence at different metallicity
Number density
Age [Gyr]
[Fe/H]
4 < R_g [kpc] < 5
6.5 < R_g [kpc] < 7.5
9 < R_g [kpc] < 10
Upper AM sequence (migrators)
Lower AM sequence (born-locally)